VOLUME I ISSUE I SPRING 2006

MSURJ

McGill Science Undergraduate Research Journal

Where Great Minds Meet pg. 3

Nobel Laureate Leon M. Lederman reviews student posters at the annual Undergraduate Research Conference in Redpath Hall

Photo by: Claudio Calligaris for McGill Faculty of Science

Table of Contents

ARTICLE **PAGE**

Message from the Dean of Science

Undergraduate students are a fundamental part of the McGill research community of today and tomorrow. The theme of our Faculty is "Learning through Discovery".

Expanding research opportunities for undergraduates is a Faculty of Science priority, and so, in September 2005, the McGill Faculty of Science created the Office for Undergraduate Research. Some of the Office's initiatives this year have included our first annual Undergraduate Research Conference in September 2005 for students to present their work, the inaugural Soup and Science luncheon series in January 2006 for professors and students to talk about research, and a new series of elective research courses for undergraduates from U0 to U3 to take inside and outside of their own departments.

Much of today's cutting-edge science takes place at the interface of two or more disciplines. It is vital that budding researchers learn to think and work in interdisciplinary terms. It is exciting to see the launch of a student research journal that covers the breadth and depth of the Faculty of Science. This journal highlights to students of one discipline what is taking place in other areas, and it also shows the voyages of interdisciplinarity upon which so many of our young scholars are already embarking.

Congratulations to the Science Undergraduate Society for this wonderful initiative, and long live the MSURJ!

Martin Grant
Dean of Science

Photograph by Claudio Callagaris

Letter From The Editors

Welcome to the first issue of the McGill Science Undergraduate Research Journal. McGill is world renowned for its high academic achievement as well as its great emphasis on research. Our university attracts the brightest and best from around the world to study at the undergraduate level each year. During this time, many of these students participate in some type of research. Whether it be as part of an honours thesis or during the summer at a laboratory, the growth of the research community at McGill and subsequently around the world is partly due to the great achievements of our young undergraduate researchers. Countless students, both current and alumni have been or are involved with groundbreaking research throughout their undergraduate educational career. Whether this research is published in a peer-reviewed academic journal or not, undergraduate research experiences must have a medium in the University community where they may be celebrated and shared.

Our goal is to promote and exhibit the world class research that comes out of the Undergraduate population to inspire others. We hope our journal will entice research interests in all facets of science. Whether you are a long time researcher or a wide-eyed freshman, we believe that the MSURJ will substantially add to the Research missions of McGill as well as impacting University life at McGill.

The MSURJ editorial board consists of 12 very intelligent hard working undergraduates who have slaved tirelessly to produce this exciting and amazing first issue of MSURJ. Together we hope you gain insight and inspiration into the fascinating undergraduate research here at McGill.

We hope you enjoy our first ever issue and look forward to publishing future installments.

Marta Filipski
Co-Creator

Jesse Pasternak
Co-Creator

Inaugural Editorial

In his 1988 Nobel Prize acceptance speech, Physicist Leon Lederman questioned, "How can we have our colleagues in chemistry, medicine and especially in literature share with us, not the cleverness of our research, but the beauty of the intellectual edifice, of which our experiment is but one brick?" When Dr. Lederman came to McGill University to present at the inaugural Undergraduate Research Day in September 2005, he brought this inspiration to many students, kindling our spirit to learn and discover through science. Presenting to a diverse audience of students, professors and non-scientists, Dr. Lederman told the story of the neutrino, a ghostlike particle that passes through everything in the universe. Indeed, even those of us who could not grasp the scientific complexities of his research appreciated the significance of his research and learned from his experiences in science.

Dr. Lederman's presentation was a reflection of the prevailing atmosphere at the Undergraduate Research Day. A showcase of multi-disciplinary undergraduate scientific research, the event brought together McGill student researchers in diverse fields and gave them a chance to present their work to their peers and professors. By giving students the opportunity to interact with their peers in other disciplines, the event created a scientific dialogue where new perspectives were constantly being discussed and incorporated into students' projects.

We hope that the inspiration of Dr. Lederman and the Undergraduate Research Day will be reflected in the McGill Undergraduate Research Journal. The Journal will give students a forum to discuss research at our level, appreciating and integrating the contributions of our peers. Above all, we hope that it will bring together the scientific community at McGill and create a nurturing environment that inspires students to think, dream and discover.

-Lopamudra Das

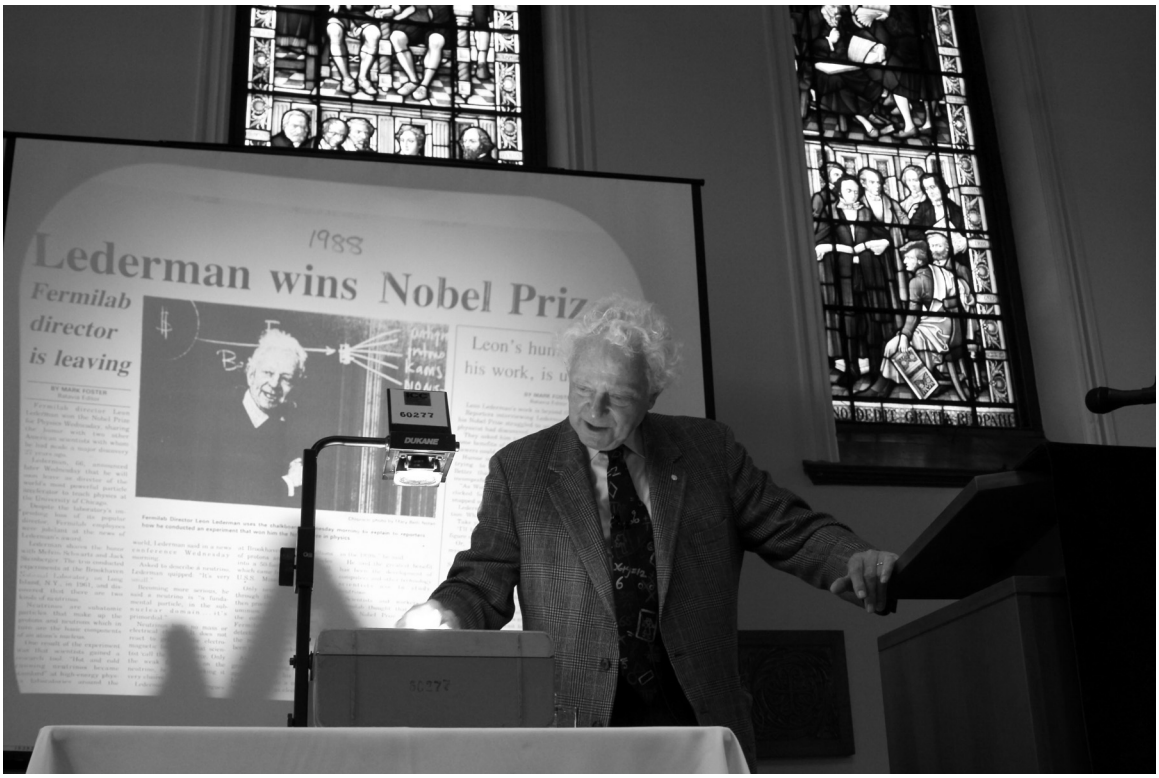

Photograph by Claudio Callagaris

The Undergraduate Research Conference

The first edition of the McGill Science Research Undergraduate Journal would not be possible without the support of the McGill Faculty of Science and its Office for Undergraduate Research (OURS). The contributions to this edition were submitted by students who participated in the first annual Undergraduate Research Conference (URC) on Friday, September 30, 2005 in Redpath Hall.

For the inaugural URC, students were nominated by each School or Department in the Faculty of Science, plus the four medical departments which offer undergraduate degrees, i.e., Anatomy and Cell Biology, Biochemistry, Microbiology and Immunology, and Physiology. There were 54 posters in total, and 58 participating students.

The MSURJ Editorial Board would like to take this opportunity to thank all the students who participated in the submission process but also congratulate award recipients of the URC.

First and second prizes were awarded in six categories as follows:

Physical Sciences

1. Shreyans Shah, *Employing the META System in Image Cross Correlation Spectroscopy: Removing Emission Bleed Through between Two Detection Channels*

Mathematical and Computational Sciences

1. Leonid Chindelevitch, *Perturbative artificial boundary conditions*
2. Christopher Hundt, *Some interesting features of convergent random variables*

Earth System Science

1. Elizabeth Anne Flanary and Sarah Anne Vereault, *Behind the Map: Predicting Marine Species' Habitat Loss Using Global Climate Models*
2. Michelle Kyle Deakin, *Crystal Growth of Diopside from a Carbonate Melt*

Biological Sciences

(Research in fundamental non-human biological processes)

1. Isabelle Racine-Miousse, *FhuD interactome: Proposing protein interactions at the bacterial cell surface*
2. Talya Hackett, *Stop, Drop or Handle: Multitasking in a Dog-Eat-Squirrel World*

Medical Sciences

(Research with clear implications for human health)

1. Vanela Bushi, *Improving Measurements of Water Proton Density in Magnetic Resonance Imaging*
2. Dominique Braidwood, *Altered perception of vertical after exposure to simulated night vision goggles*

Health and Social Sciences

(Health services research, research on humans as social cultural beings; research on the economic, political, social and cultural dimensions of human activity)

1. Christian Webb, *Materialistic Values and Well-Being: A Multi-Wave Longitudinal Analysis by Latent Interaction Models*
2. Thien Kim Nguyen, *The role of compensatory health beliefs and self-efficacy on treatment adherence in adolescents with Type 1 diabetes*

Sediment Geochemistry In The Canadian Arctic

Carole Gilbert, Alfonso Mucci, and Bjorn Sundby

Department of Earth and Planetary Sciences, McGill University, 3450 University St., Montreal, Quebec, Canada, H3A 2A7
Correspondence should be addressed to Carole Gilbert : carole@eps.mcgill.ca

Given the current threat of fast-paced global change, it has become urgent to understand the biogeochemical response of the Arctic environment to external forcing. The Canadian Arctic Shelf Exchange Study (CASES) is an interdisciplinary project put together by scientists from across Canada whose primary goal is to gain a better understanding of the Canadian Arctic environment. Objectives include evaluating issues such as the impact of climate change – extent of sea ice cover - on biological productivity and the carbon cycle. In order to predict the potential evolution of the complex Canadian Arctic system, the intricacies of its current dynamics must first be understood.

This study focuses on the geochemical characteristics of the sediments in the Canadian Arctic shelf. A series of sediment cores taken at various locations in the Beaufort Sea and Amundsen Gulf (fig. 1) were analyzed for reactive solid-phase manganese and iron oxides. These data were used to determine the redox zonation and availability of electron-acceptors within the sedimentary column. The abundance and vertical distribution of the metal oxides reflect a history of organic carbon delivery to the seafloor. Manganese and iron are the focus of this study because they contribute significantly to the oxidation of the organic matter (OM) reaching the seafloor and are abundant in the Earth's crust. By combining data on organic carbon content and dissolved manganese and iron, spatial correlations were established and the variations in sedimentary geochemical environments were interpreted across the study area.

Key Terms

Forcing:
A persistent disturbance of a system (longer term than perturbation).

Redox zonation:
availability of electron-acceptors within the sedimentary column

Sedimentary column:
vertical section of sediment at a given location

Oxidizing conditions:
in the presence of oxygen

Reducing conditions:
in the absence of oxygen

Diagenesis:
any change undergone by sediment after deposition

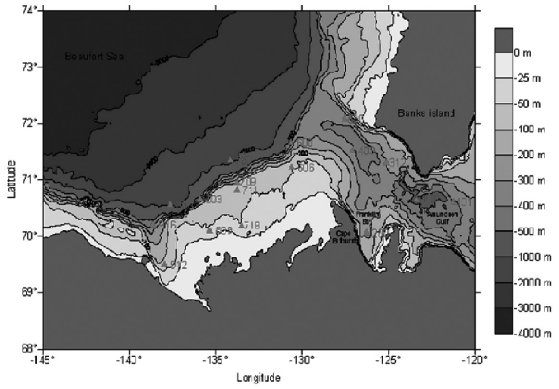

Figure 1. Location of the Beaufort Sea and Admunsen Gulf with respect to the Canadian Northwest Territories. Triangles represent sampling stations.

Laboratory work focused on sediment recovered from cores sub-sampled (at predetermined depth intervals) on-board the CCGS Amundsen in 2003-2004. The freeze-dried sediments were homogenized and the abundance as well as the vertical distribution of reactive iron and manganese minerals was determined according to methods described by Kostka and Luther (1994) and Leventhal and Taylor (1990), using buffered ascorbate- and HCl-extractable phases for their extraction. Manganese (Mn) and iron (Fe) dissolved by these reagents and the sediment porewaters were analyzed by atomic absorption spectroscopy using an air-acetylene flame.

The vertical distribution of solid and dissolved phases of Mn and Fe in the sediment is largely dependant on whether or not oxygen is present in the sediment and exactly how deep it can penetrate. The oxygen penetration depth (OPD) is mainly a function of bottom water oxygen concentration and OM input and reactivity. Oxygen oxidizes organic matter in reactions mediated by bacteria. The higher the input of OM and the more reactive it is, the more rapid

is the consumption of oxygen. The more rapidly oxygen is consumed, the shallower the depth of oxygen penetration. The OM discussed here is derived from a combination of two sources: continental (i.e. Northwest Territories via the Mackenzie River) and the marine environment (i.e. Arctic surface waters). Typically, marine OM is more reactive than continental OM due to its lower carbon to nitrogen ratios.

The OPD is reflected in the distribution of Mn and Fe because these elements, delivered by settling particulate matter, are insoluble under oxidizing conditions and soluble under reducing conditions. The depth in the sediment that separates these two situations is called the redox boundary. For a given sediment sample the redox boundary and OPD occur at the same depth. A sharp increase in the concentrations of the dissolved, reduced forms characterizes the redox boundary (fig. 2). The elemental concentration gradients across this boundary drive a diffusive flux of soluble, reduced Mn and Fe upward. Upon encountering dissolved oxygen, soluble Mn and Fe precipitate as oxides and accumulate near the OPD. With time, as a result of continuous sedimentation, these oxides are buried below the redox boundary and are dissolved again via reduction. The net result is that Mn and Fe cycle across their respective redox boundaries. These boundaries are typically observed at depths varying between 5 and 25 cm in the Canadian Arctic.

The depth of the redox boundary is important because the closer it is to the sediment water interface, the higher the probability that dissolved metals may escape the sediment and get carried offshore by ocean currents, to be later deposited in the deep sea. In other words, the redox cycle is not necessarily confined to the sediment but may also include the water column.

The examination of several of these profiles has led to the conclusion that there are two distinct geochemical environments operating in the Canadian Arctic: The Admunsen Gulf/ Abyssal Plains of the Beaufort Sea, and

the Mackenzie Shelf. The former is characterized by extremely high concentrations of reactive Fe and Mn, low sedimentation rates, low concentrations of poorly reactive organic carbon and a redox boundary located deep within the sediment (fig. 2). In contrast, the Mackenzie Shelf environment is characterized by low Fe and Mn concentrations, high sedimentation rates, elevated concentrations of highly reactive OM and a redox boundary close to the sediment-water interface. On the Mackenzie

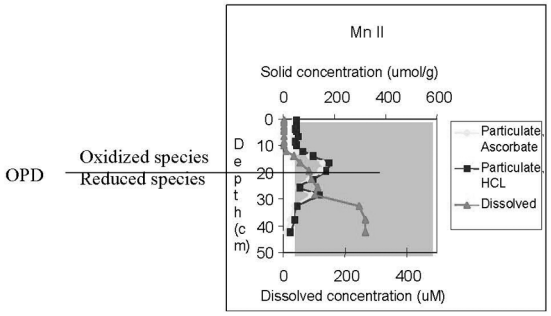

Figure 2. Sample Mn profile taken in the Beaufort Sea (Station 750) illustrating the position of the redox boundary.

Shelf, diagenesis is fueled by a high influx of OM (sediment input from the continent), which brings the redox boundary for manganese and iron closer to the sediment-water interface.

This allows dissolved species to escape the sediment and to get carried offshore. Here, the dissolved species are re-oxidized in the water column and re-deposited in the Admunsen Gulf and Abyssal Plains of the Beaufort Sea.

The results in this study contribute to the advancement of CASES' objectives. From these results it can be speculated that increased global warming may increase precipitation over Canada, leading to higher weathering rates and greater sediment deposition onto the Mackenzie Shelf. Consequently, the redox boundary on the Mackenzie Shelf may thin even more, allowing a larger quantity of dissolved species to escape the water column and to be transported into the deep environment. In addition, the increased delivery of nutrients by the river and the decreasing ice cover may lead to greater primary production and the delivery of more reactive OM to the seafloor; once again thinning the oxidizing layer. It is generally believed that the Arctic is particularly fragile and sensitive to change, though this is still a hot topic for debate and has yet to be determined empirically.

Special thanks to Gwenaelle Chaillou and Cedric Magan for their guidance and input in the realization of this project.

References

1. Gagnon C., A. Mucci and E. Pelletier (1995) Anomalous accumulation of acid-volatile sulphides in a coastal marine sediment (Saguenay Fjord, Canada). Geochim. Cosmochim. Acta 59, 2663-2675.
2. Kostka, J.E. and G.W. Luther (1994) Partitioning and speciation of solid phase iron in salt marsh sediments. Geochim. Cosmochim. Acta 58, 1701-1710.
3. Leventahl J. and C. Taylor (1990) Comparison of methods to determine degree of pyritization. Geochim. Cosmochim. Acta 54, 2621-2625.

The Role of Compensatory Beliefs and Self-efficacy on Treatment Adherence in Adolescents with Type 1 Diabetes

Thien-Kim Nguyen, Dr. Bärbel Knäuper & Marjorie Rabiau

Abstract

Many adolescents suffering from type 1 diabetes have difficulty following the strict demands of their treatment, which can lead to serious health complications. Previous research has shown that self-efficacy, or the conviction that one can achieve a certain goal, has a positive effect on adherence to treatment. We propose that compensatory beliefs (CBs) also have a significant impact on the adherence to treatment which explains why diabetic teenagers fail to fully adhere to their proposed treatment. In a sample of 115 diabetic adolescents, inaccurate compensatory beliefs significantly correlated with poor glycemic control, self-reported blood-sugar monitoring and diet. However, self-efficacy did not significantly correlate with CB levels and accurate compensatory beliefs were not significantly linked of many of the measures of treatment adherence.

Introduction

Type 1 diabetes is the most common endocrine disorder in children and adolescents (Canadian Diabetes Association (CDA), 2003). The main differences between type 1 and type 2 diabetes is that the former develops during childhood and is characterized by a total lack of insulin, whereas the latter's onset is typically in adulthood and is associated with having too little insulin or failing to metabolize insulin efficiently. Patients with type 1 diabetes must get insulin injections on a regular basis because their body fails to produce this hormone, essential for the regulation of blood-sugar levels. However, insulin administrations alone are not sufficient to manage the disorder because several other behavioral variables that affect blood-sugar levels need to be monitored as well. To manage diabetes properly, patients need to watch their diet, to exercise, to control stress levels and to monitor their blood-sugar. Previous research indicates that adolescents with type 1 diabetes have special difficulty following the strict demands of the treatment; hence, they are at high risk of developing further health complications that may lead to hospitalization (Bougneres et al., 1993).

Why do diabetic adolescents have such difficulty adhering to their treatment? One possible hypothesis is that type 1 diabetic adolescents engage in compensatory beliefs (CBs). Compensatory beliefs are convictions that the negative effects of an unhealthy behavior can be compensated for by engaging in a healthy behavior (Knäuper, Rabiau, Cohen, & Patriciu, 2004). An example of a compensatory belief that is applicable to the general population is "Exercising at the gym will compensate for eating this cookie". Other CBs that are directly related to diabetes include "Taking extra insulin can make up for the increase in blood glucose caused by eating an extra snack" and "Drinking milk compensates for an increase in blood-sugar caused by eating too many sweets". Rabiau, Knäuper, and Miquelon (2005) have theorized that CBs are produced when one is in a state of discomfort because of a temptation to engage in an unhealthy behavior. This uneasy feeling is triggered by the conflict between the goal to stay healthy and a temptation (i.e. eating sweets). In order to relieve this motivational conflict, CBs are activated and allow the person to engage in the unhealthy behavior by reducing the feelings of uneasiness. Thus, CBs may prevent type 1 diabetes adolescents from fully adhering to their treatment because they reduce the patients' guilt when they engage in unhealthy behaviors (e.g. not taking their insulin).

Another important concept often associated with health behaviors is self-efficacy. Self-efficacy is the belief that one can carry out specific tasks and attain certain goals (Bandura, 1977). Previous literature has suggested that diabetic

patients with low self-efficacy will fail to handle the stresses of their illness, to administer insulin regularly, to plan their meals properly and to exercise regularly (Grossman, Brink, & Hauser, 1987). Rabiau et al. (2005) further posit that people with low self-efficacy are more likely to engage in maladaptive CBs because they lack the self-control that is necessary to follow their health goals.

Although CBs may be efficient at reducing guilt, they may harm the diabetic patient's health in two specific circumstances: (1) when a patient does not implement the compensatory behavior involved in the CB that follows treatment recommendations (i.e. a diabetic boy forgets to inject the extra insulin to make up for the rise in blood sugar caused by eating an extra snack), and (2) when a patient acts based on CBs that are in contradiction with treatment recommendations (i.e. drinking milk cannot compensate for eating too many sweets because implementation of this compensatory behavior will further increase blood sugar levels instead of decreasing them) (see Figure 1). CBs that are in accordance with treatment recommendations are called "accurate" CBs, whereas those that are in contradiction with the recommendations are appropriately named "inaccurate" CBs. Another category of CBs are sugar-testing CBs, which are beliefs related to blood-sugar monitoring (i.e. "Testing my glucose twice in the afternoon can make up for not testing my glucose in the morning"). Sugar-testing CBs are particularly interesting as they are extremely inaccurate beliefs and should, therefore, inevitably lead to poor glycemic control. In other words, they are a specific subtype of inaccurate CBs which are most likely to be used by diabetic adolescents who are most at-risk for developing heath complications.

The objective of the present study is to investigate whether CBs and self-efficacy could further explain why adolescents with type 1 diabetes have difficulty following their treatment regime. If CBs are linked with poorer treatment adherence, we might integrate them as part of the education process of diabetic patients to help improve their health. We hypothesized that (1a) lower self-efficacy will be associated with higher levels of inaccurate diabetes-specific CBs, and (2a) higher levels of inaccurate diabetes-specific CHBs will be linked with lower treatment adherence. Furthermore, we expected that (1b) higher levels of self-efficacy will be associated with higher levels of accurate diabetes-specific CBs, and (2b) higher levels of accurate diabetes-specific CBs will be linked with higher adherence to the treatment regime.

Figure 1. When Are CHBs Unhealthy?

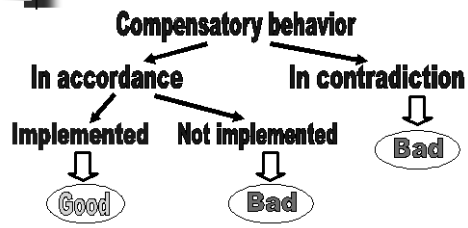

Method

In order to test our hypotheses, we administered a questionnaire to a sample of 115 adolescents aged 12 to 18 with type 1 diabetes from the Montreal Children's Hospital Diabetes Clinic. More specifically, we asked the participants to fill out the questionnaire while they waited for their appointment with the doctor at the waiting room of the clinic. The 45 minute questionnaire included: (1) the Diabetes CB scale, developed by Rabiau, Knäuper and Nguyen (2006, submitted), in which participants rated on a scale from 1 to 5 the extent to which they agreed with a certain compensatory belief (i.e. "Having a juice before exercising can make up for the decrease in blood glucose caused by the exercising"), (2) the Diabetes Self-efficacy scale, developed by Rubin and Peyrot (1989), which measures the degree of the participants' conviction that they can carry out a certain task (i.e. "How sure are you that you can judge the amount of food you should eat before activities?"), and (3) the Diabetes Self-Care Activities scale, developed by Toobert, Hampson and Glascow (2000), which is the self-reported measure of adherence to treatment and contains questions on different aspects of diabetes self-management (i.e., diet, exercise, blood-sugar testing, and smoking).

In addition to the self-reported measure of treatment adherence, we obtained the patients' glycosylated hemoglobin test results (HbA1c) from their medical files to get a physiological measure of the extent to which they follow their treatment. We used the HbA1c test result on the day that the patient participated in our study. HbA1c test results reflect the patients' average glycemic control over the past three months before the test. More specifically, the HbA1c test shows the percentage of sugar attached to hemoglobin — the substance that carries oxygen in red blood cells. The higher the amount of sugar in the bloodstream, the more sugar molecules will stick to hemoglobin and remain there for red blood cell's entire lifespan, which is normally three months. In other words, the hemoglobin gets "glycosylated". High HbA1c results suggest poor control over blood sugar and low adherence to treatment.

Results

To verify our predictions about the relationships between self-efficacy, CBs and treatment adherence, we correlated (1) the self-efficacy scores with the different CB subscales (i.e., accurate, inaccurate, and blood-sugar testing CBs) and (2) the different CB subscales with the measures of treatment adherence (i.e., both self-reported and glycemic control). Although we did not find significant correlations between diabetes self-efficacy and the CB subscales, they all followed the direction that we expected (i.e., high self efficacy was associated with high levels of accurate CBs and low levels of inaccurate and sugar-testing CBs).

Sugar-testing CBs were the only CBs that significantly correlated with HbA1c ($r = .27$, $p = .01$, two-tailed) (see Figure 2), which partially supports our predictions r egarding the different CB subscales and the physiological measure of treatment adherence. Remember that high levels of HbA1c indicate low glycemic control, and vice-versa. Thus, high levels of sugar-testing CBs are linked with high glycosylated hemoglobin test results, which suggest poor adherence to treatment. Despite the fact that the other CB subscales did not significantly correlate with the HbA1c test results, they all followed the expected direction of relationships (i.e., high levels accurate CBs are linked with low HbA1c, while high levels of inaccurate CBs are associated with high HbA1c).

Figure 2

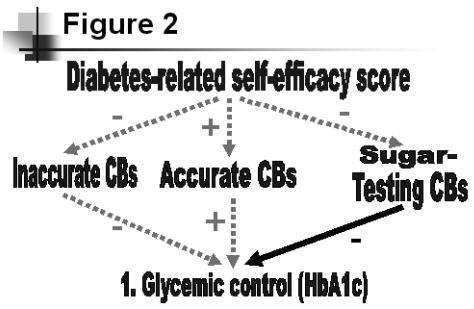

We also found that inaccurate and sugar-testing CBs had strong negative correlations with both self-reported diet and sugar-testing. In fact, the specific diet subscale significantly correlated with inaccurate CBs ($r = -.37$, $p < .01$, two-tailed) and blood-sugar testing CBs ($r = -.28$, $p < .01$, two-tailed) (see Figure 3). Self-reported blood-sugar testing significantly correlated with inaccurate CBs ($r = -.41$, $p < .01$, two-tailed) and blood-sugar testing CBs ($r = -.50$, $p < .01$, two-tailed). Contrary to our predictions, none of the CB subscales significantly correlated with self-reported exercise and smoking. Considering that only 6.1% of the participants claimed that they smoked at least one cigarette for the past seven days, it was very difficult to find a significant correlation for the smoking status subscale.

Figure 3

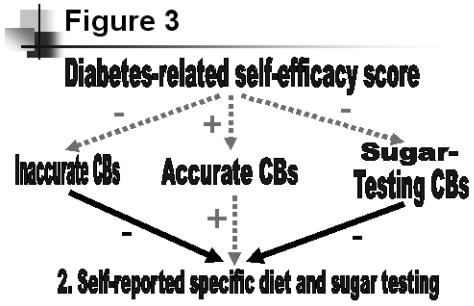

Contrary to our expectations, accurate CBs did not significantly correlate with any of the measures of treatment adherence. On second thought, this result may make sense because accurate CHBs can lead to both successful and unsuccessful glycemic control (refer back to Figure 1). In fact, regulation of blood-sugar levels depends on the success or failure to implement the compensatory behavior involved in the CB. If the CB in question is accurate (i.e. "Exercising can make up for the change in glucose caused by stress"), implementation of the compensatory behavior (i.e., exercising) will result in good glycemic control, while failure to implement the behavior (i.e., forgetting to exercise) leads to poor regulation of blood glucose. To put it differently, accurate CBs may have weakly correlated with physiological and self-reported measures of treatment adherence because they can result in opposite effects on health.

In summary, contrary to our predictions, self-efficacy did not significantly correlate with any of the CB subscales. This finding may be due to the fact that the participants' self-efficacy scores were high and were relatively narrow in distribution ($M = 4.29$ on a 5-point scale, $SD = 0.47$), which may suggest a ceiling effect. In fact, it is often difficult to find significant correlations when the means of the variables are extremely high or low and when the scores all concentrate around a certain value. However, in support of our hypotheses, maladaptive CBs (namely, blood-sugar testing CBs) were strongly associated with lower glycemic control and poorer habits concerning blood-sugar monitoring and specific diet. These results imply the importance of raising awareness about these maladaptive CBs (i.e., through discussions with medical professionals or through the use of pamphlets) to help type 1 diabetes adolescents improve their treatment adherence and achieve better health.

Conclusion

A limitation of the present study is that the data cannot show the direction of the relationships between the variables. For instance, we cannot prove in exact order that low self-efficacy leads to more CBs, which in turn leads to lower adherence to treatment. However, future research could deal with the problem of causal direction. As a follow-up study, type 1 diabetes adolescents who have particular difficulty adhering to the treatment (i.e. those with high HbA1c levels) could be given a portable pocket-sized computer and be asked to answer questions several times during the day. The participants could be asked to describe the most recent temptation that they encountered (i.e. not testing blood-sugar levels because of being late for school) and write about their thoughts and how they dealt with this temptation. This experience sampling method could help solve the issue of causal direction because it shows the patients' sequence of thoughts. Future research (which could use this experience-sampling method as well) could also include studying CBs in other populations, such as dieters and type 2 diabetes patients. For example, dieters may fail to lose weight because they resort on the belief that "Eating dessert can be made up by skipping the main dish". If we find that such beliefs are linked with either adverse or beneficial health effects, educating people about which CBs are adaptive or maladaptive would be important to help them achieve a healthier lifestyle.

References

1. Bandura, A. (1977). Self-efficacy: Toward a unifying theory of behavioral change. Psychological Review, 84, 191-215.

2. Bougneres, P. F., Landais, R., Mairesse, A. M., Jais, J. P., Jos, J., Peyraud, J., Wieliczko, M. C., Chavoix, P., Garandeau, P., Asensi, D., Ythier, H., Rouland, V., Mazoyer, T., Leturcq, F., & Raynaud, E. (1993). Improvement of diabetic control and acceptability of a three-injection insulin regimen in diabetic adolescents. Diabetes Care, 16, 94-102.

3. Canadian Diabetes Association (2003). 2003 clinical practice guidelines for the prevention and management of diabetes in Canada. Canadian Journal of Diabetes, 27, S84.

4. Grossman, H. Y., Brink, S. J., & Hauser, S. T. (1987). Self-efficacy in adolescent girls and boys with insulin-dependent diabetes mellitus. Diabetes Care, 10, 324-329.

5. Knäuper, B., Rabiau, M., Cohen O., & Patriciu, N. (2004). Compensatory health beliefs: Scale development and psychometric properties. Psychology & Health, 19(5), 607-624.

6. Rabiau, M., Knäuper, B., & Miquelon, P. (2005, in press). The eternal quest for optimal balance between maximizing pleasure and minimizing harm: The Compensatory Health Beliefs Model. British Journal of Health Psychology.

7. Rabiau, M., Knäuper, B., & Nguyen, T. (2006, submitted). Psychometric properties of a diabetic-specific compensatory beliefs scale for adolescents. Health Psychology.

8. Rubin, R. R., & Peyrot, M. (1989). Effect of diabetes education on self-care, metabolic control, and emotional well-being. Diabetes Care, 12, 673-679.

10. Toobert, D.J., Hampson, S.E., & Glascow, R. E. (2000). The summary of diabetes self-care activities measure. Diabetes Care, 23, 943-950.

Mercury Determination: A Hair Raising Experiment

David Duford[a], Josiane P. Lafleur[a], Rebecca Lam[a], Cameron D. Skinner[b] and Eric D. Salin[a]

[a]Department of Chemistry, McGill University, 801 Sherbrooke St. W., Montreal, Quebec, Canada H3A 2K6.
[b]Department of Chemistry & Biochemistry, Concordia University, 7141 Sherbrooke St. W., Montreal, Quebec, Canada, H4B 1R6.
Correspondence should be addressed to Eric D. Salin: eric.salin@mcgill.ca

Abstract

A novel, fast, low-cost portable system for the total analysis of mercury (Hg) in human hair is presented by induction heating-electrothermal vaporization, gold amalgamation, atomic absorption spectrometry (IH-ETV-GA-AAS). Using this innovative technique a detection limit of 1 ng (or 1.5 mg/g based on a 0.6 mg sample) was achieved.

Introduction

Mercury (Hg) has for centuries been a useful metal in a variety of applications. Unfortunately this usefulness is counterbalanced by its neurotoxicological health impact. Hg is introduced in the food chain when anaerobic bacteria at the bottom of the bodies of water convert inorganic Hg into an organic Hg form. Progressively larger and larger life forms consume the former as part of the natural food chain, essentially concentrating the Hg (Skoog, West and Holler 1996). Some aquatic life concentrates Hg by a factor of 100,000 leading to dangerous levels as high as 20 parts per million (ppm) in some potentially commercialized fish intended for human consumption. For these reasons, the American Food and Drug Administration (FDA) has set a legal limit of one ppm and Health Canada an even lower 0.5 ppm limit for fish intended for human consumption. Likewise, these organizations have issued an advisory to women who may become pregnant, pregnant women, nursing mothers, and young children to avoid some types of fish and eat fish and shellfish that are lower in mercury (Health Canada 2004; Rados 2004).

In view of the above, analytical methods play an important role maintaining quality control, minimizing the health impact of Hg. The analysis of human hair has been proven to be reflective of the body's total Hg load (Legrand et al. 2005) and obviously is less intrusive than blood tests (Barbosa et al. 2004). Conventional methods for the determination of Hg in hair include cold-vapour atomic absorption spectrometry (CV-AAS) (Manzoori, Sorouraddin and Haji 1998), cold-vapour atomic fluorescence spectrometry (CV-AFS) and inductively coupled plasma mass spectrometry (ICP-MS) (Gill, Schwartz and Bigras 2002). These methods require about 5 to 10 mg of hair (some 100 strands of hair) and include a lengthy digestion step (which introduces the potential for contamination and loss). To minimize the quantity of hair needed as well as remove the digestion step, direct Hg analyses of human hair strands have been performed by X-ray fluorescence (Toribara and Jackson 1982), particle induced X-ray emission spectroscopy (Valkovic et al. 1973), and laser ablation-inductively coupled mass spectrometry (LA-ICP-MS) (Legrand et al. 2004). These techniques have the advantage of little sample preparation yet are limited by detection limit, expensive instrumentation or difficult calibration. Alternatively, combustion gold amalgamation atomic absorption spectroscopy (C-GA-AAS) has been used for the direct analysis of hair, yet still requires some sample preparation involving the addition of a catalyst (to promote combustion) and modifiers (to absorb combustion by-products) (Cizdziel and Gerstenberger 2004; Legrand et al. 2004). Most recently, induction heating-electrothermal vaporization inductively coupled plasma mass spectrometry (IH-ETV-ICP-MS) was employed for direct analysis of total mercury in a single human hair strand, achieving a detection limit of 20 pg or 30 ng/g (based on a 0.6 mg sample) (Lafleur et al. 2005). The primary disadvantage with this system is its costly and bulky detection system.

Key Terms

Mercury

Human hair

Induction heating electrothermal vaporization

Gold amalgamation

Atomic absorption

We report here an alternative method that is fast, less costly and potentially field portable which combines the simple direct sample vaporization of induction heating-electrothermal vaporization, with a gold amalgamation trap and detection at 253.7 nm by atomic absorption spectrometry (IH-ETV-GA-AAS). This system could be very useful in monitoring Hg exposure in populations at risk such as Native North American fishing populations.

Materials and Methods

Induction heating-electrothermal vaporization (IH-ETV) sample introduction

The IH-ETV sample introduction system has previously been described in detail (Goltz and Salin 1997; Goltz, Skinner and Salin 1998; Rybak and Salin 2001). In previous work, it has been used to vaporize soil slurries (a liquid mixture of water and insoluble matter), cellulose filters and human hair (Rybak and Salin 2001; Salin and Ren 2003; Lafleur et al. 2005). As seen in Figure 1, the IH-ETV consists of a modified "Leco" induction furnace. The samples were placed in commercially available graphite sample cups equipped with boiler caps to prevent the escape of the sample. These graphite cups were placed at the center of the induction coil of the modified furnace which, when turned on, heated the cups without any physical contact and vaporized the sample (in this case hair). The vaporized samples were entrained out of the IH-ETV by an argon (Ar) gas stream through PTFE tubing at a flow rate of 500 mL/min. Furthermore, to eliminate undesirable arcing between the graphite cup and the surrounding quartz chamber (which would char the graphite cup and introduce undesirable particles in the carrier gas stream), water vapour was introduced by the use of a sparger (Ren, Rybak and Salin 2003).

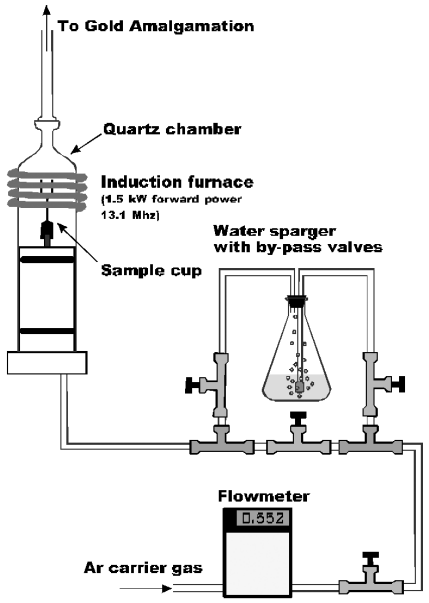

Figure 1. Schematic of the sample introduction Induction Heating-Electrothermal Vaporization (IH-ETV) with water sparged option of argon carrier gas.

The primary advantage of this sample introduction technique was the removal of all sample preparation steps from the assay. This corresponded to a reduction in time and risk of contamination.

The temperature of the graphite cups versus applied voltage was determined by the use of calibrating lacquers and pellets. The applied voltage was varied using a variable transformer. A linear relationship between the applied voltage and the resulting temperature of the graphite cups was observed thus permitting the user to set the desired temperature of vaporization.

Gold Amalgamation Trap (GA)

Gold and Hg have for years been linked by their unique capability to form an amalgam (alloy or mixture of two or more metals) at room temperature. This amalgam is however thermally unstable above approximately 3500C (Aeschliman and Norton 1999).

Based on this information, a gold amalgamation trap for Hg could be designed. Several set-ups have been documented. The source of the gold ranges from gold-sintered silica or gold sintered diatomaceous earth (Takaya and Kohyama 2004), gold-coated sand (Dumarey, Dams and Hoste 1985; Liang and Bloom 1993), gold sponge, to gold sputter-coating on quartz wool (Aeschliman and Norton 1999; Slemr et al. 1979). Heating the traps by means of a tube furnace (Aeschliman and Norton 1999), heating lamps (Takaya and Kohyama 2004) and nichrome heating wire (Liang and Bloom 1993; Slemr et al. 1979) have been documented. A simple yet effective adaptation of these was developed and constructed using powdered gold and nichrome heating wire as seen in Figure 2. Likewise it has been shown that gold traps can reproducibly collect nearly 100% of all types of Hg (organic and inorganic), provided that the sample does not exceed the limit of a given trap, related to the exposed gold surface area (Brosset, and Iverfeldt 1989).

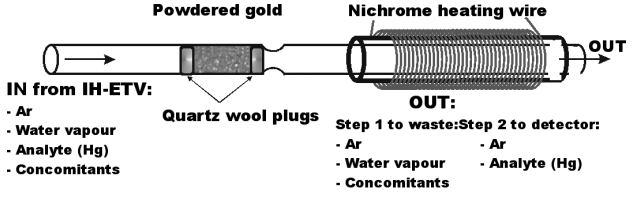

Figure 2. Schematic of the gold amalgamation (GA) trap

The output mixture of the IH-ETV entered the gold trap at one end. At this point the mixture was composed of the inert argon carrier gas, water vapour, the Hg analyte and other concomitants (everything other than the Hg analyte). At room temperature the gold (99.99% purity) theoretically only retained the Hg by the formation of an amalgam. The water vapour and concomitants which were not retained by the gold were swept through the system and were either sent directly to waste or were observed at an early retention time. Meanwhile, the resistance heating nickel-chromium wire was preheated to about 6000C. This high temperature was more than sufficient to rapidly liberate the Hg from the gold (Aeschliman and Norton 1999). Once sufficient time had passed to eliminate the water vapour and other concomitants which would have interfered with the absorption reading, the red-hot resistance heating wire was quickly moved over the gold. Within seconds, the gold trap was heated liberating the Hg from the gold. The Hg (now concentrated) was swept by continuously flowing argon to the detection system. The system was purged between runs to insure that the trap was free of Hg by alternating between blank and sample runs.

Atomic Absorption Spectrometry (AAS)

The detection system used was a simple configuration formerly built in-house. As seen in Figure 3, the atomic absorption spectrometer was comprised of a Hg pen lamp whose UV emission wavelength at 253.7 nm was collimated (light whose rays are parallel) by a quartz lens (Ingle and Crouch 1988). A glass cell equipped with two quartz windows with a 20 cm path length was used. The Hg analyte being carried out of the gold trap by the argon gas passed through this cell where absorption could take place. At the other end, another quartz lens focused the transmitted light onto a 25 mm2 UV-enhanced silicone photodiode equipped with a 254 nm filter. The resulting spectra were recorded on a strip chart and via an A/D converter on computer to facilitate data treatment and analysis. The measured transmittance was subsequently converted to absorption in order to relate the latter to concentration via Beer-Lambert law, (A = ebc).

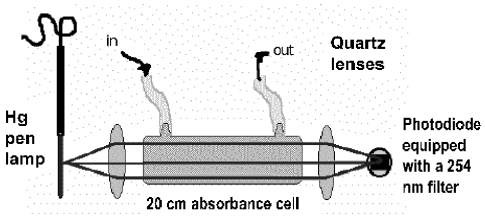

Figure 3. Schematic of the atomic absorption spectrometer (AAS)

Standards, reagents and samples

Standard solutions were prepared by consecutive dilutions of a Hg stock solution, with 1% trace metal grade nitric acid in Milli-Q water (18 MW distilled deionized water). All standards were stored in polypropylene containers (Nalgene) that had been preconditioned with 10 % trace metal grade nitric acid for a period of 24 hours and rinsed with distilled deionized water.

The hair samples came from women living in the village of Brasilia Legal, Brazil. Details of this population and hair collection procedures are described elsewhere (Passos et al. 2003). As part of two other interdisciplinary projects, the mercury concentrations of 12 cm segments of these hair strands were previously determined by CV-AAS (Legrand et al. 2005) and C-GA-AAS (Passos et al. 2003). For this study, hair strands were cut to a 12 cm length from the root end and weighed to the nearest 0.01 mg.

Results and Discussion

Assays were first performed without the gold amalgamation (GA) trap. The liquid Hg standards resulted in a linear calibration plot. However when the standardized hair samples were ran, very large absorbencies were observed as well as a notable baseline drift. These occurrences may be due to the presence of water vapour or other concomitants in the observation cell during the reading, causing erroneous absorbance or scattering. To simultaneously purify, preconcentrate and delay the Hg signal (till the baseline restabilized), the GA trap was introduced.

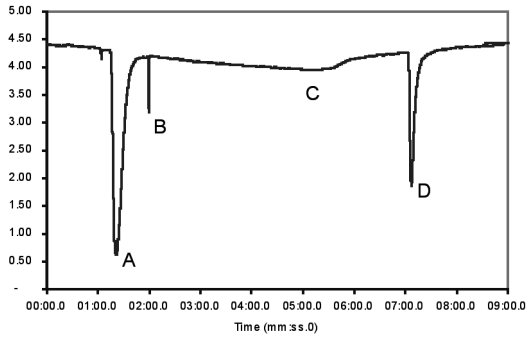

Figure 4. AA) spectrum of a single hair strand (10 pt moving avg) A) Concomitants, B) electronic noise, C) baseline drift, D) Hg analyte

The liquid Hg standards and standardized single hairs were again analyzed. A 10 point boxcar moving average (a smoothing technique) was applied to the acquired spectra. Peak heights were used and the corresponding

absorbencies determined according to Beer's Law. A calibration plot using the liquid Hg standards revealed a linear plot with a detection limit of 1 ng or 1.5 mg/g (based on a 0.6 mg sample hair mass) The spectrum of one of the analyzed hairs can be seen in Figure 4. Of note was the large peak A at 1:00 minute, no doubt due to water vapour and other concomitant. Peak B at 2:00 minutes was due to electronic noise when the IH-ETV switch was depressed. Furthermore, the baseline drifted significantly as before (region C) and consequently was allowed time to stabilize. At the 7 minute mark, the red hot coil was quickly moved over the gold, at which point the Hg was released from the gold and swept by the flowing Ar gas to the detection system and recorded as peak D.

It was thus demonstrated that the gold amalgamation trap successfully retained the Hg. However, the peak height (or peak area) were much larger than expected compared to the liquid standards. Unfortunately there seemed to be other concomitants that were also retained by the gold trap. At this point only speculations to the identity of these concomitants are made, but they were probably organic compounds from the vaporized hair which inherently would scatter the light and absorbed in the approximate region surrounding 254 nm (Ingle and Crouch 1988).

Conclusion

The potential for a low-cost system for the analysis of Hg in human hair by induction heating electrothermal vaporization, gold amalgamation, atomic absorption spectrometry (IH-ETV-GA-AAS) was demonstrated. With its demonstrated characteristics, such as linear temperature control, sample purification and preconcentration, one nanogram detection limit for Hg, and digital acquisition, this system has the potential to be made into a low cost, field portable system capable of monitoring populations at risk due to dietary or work exposure to Hg. The main focus of future work shall be the use of atomic fluorescence spectrometry (AFS) and/or an atomic absorption system with a continuum source background correction system (AAS-BC) to overcome the presence of organic species, to account for scattering and to minimized drift.

Acknowledgements

Scholarship support from the Natural Sciences and Engineering Research Council (NSERC) Undergraduate Student Research Award (USRA) is gratefully acknowledged by David Duford.

References

Aeschliman, D.B. and G.A. Norton. 1999. Collection and Thermal Evolution Behaviors of Different Mercury Species Captured with Gold. Environ. Sci. Technol. 33: 2278-2283.

Barbosa, F., C.D. Palmer, F. J. Krug and P.J. Parsons. 2004. Determination of total mercury in whole blood by flow injection cold vapor atomic absorption spectrometry with room temperature digestion using tetramethylammonium hydroxide. J. Anal. At. Spectrom. 19: 1000-1005.

Brosset, C. and A. Iverfeldt. 1989. Interaction of solid gold with mercury in ambient air. Water, Air, and Soil Pollution 43: 147-68.

Cizdziel, J.V. and S. Gerstenberger. 2004. Determination of total mercury in human hair and animal fur by combustion atomic absorption spectrometry. Talanta 64: 918-921.

Dumarey, R., R. Dams and J. Hoste. 1985. Comparison of the Collection and Desorption Efficiency of Activated Charcoal, Silver, and Gold for the Determination of Vapor-Phase Atmospheric Mercury. Anal. Chem. 57: 2638-2643.

Gill, U.S., H. M. Schwartz and L. Bigras. 2002. Results of Multiyear International Interlaboratory Comparison Program for Mercury in Human Hair. Arch. Environ. Contam. Toxicol. 43: 466-472.

Goltz, D.M. and E. D. Salin. 1997. Inductively Heated Vaporizer for Inductively Coupled Plasma Mass Spectrometry. J. Anal. At. Spectrom. 12: 1175-1180.

Goltz, D.M., C.D. Skinner and E.D. Salin. 1998. Sample introduction for inductively coupled plasma atomic emission spectrometry using an inductively heated vaporizer. Spectrochim. Acta, Part B 53B: 1139-1147.

Health Canada. 2004. Mercury and the Environment. http://www.ec.gc.ca/MERCURY/EH/EN/eh-hc.cfm?SELECT=EH (accessed January 6, 2006).

Ingle, J.D. and S, R. Crouch. 1988. Spectrochemical Analysis. New Jersey: Prentice Hall, 50, 95, 113, 127-8, 140, 174, 280-1, 336.

Lafleur, J.P., R. Lam, H.M. Chan and E.D. Salin. 2005. Induction heating-electrothermal vaporization for direct mercury analysis of a single human hair strand by inductively coupled plasma mass spectrometry. J. Anal. At. Spectrom. 20: 1315-1317.

Legrand, M., C. J. S. Passos, D. Mergler and H. M. Chan. 2005. Biomonitoring of Mercury Exposure With Single Human Hair Strand. Environ. Sci. Technol. 39: 4594-4598.

Legrand, M., R. Lam, M. Jensen-Fontaine, E. D. Salin and H. M. Chan. 2004. Detection of Mercury in Single Human Hair Strands by Laser Ablation Inductively Coupled Plasma Mass Spectrometry. J. Anal. At. Spectrom. 19: 1287-128.

Liang, L. and N.S. Bloom. 1993. Determination of total mercury by single-stage gold amalgamation with cold vapor atomic spectrometric detection. J. Anal. At. Spectrom. 8: 591-4.

Manzoori, J.L., M. H. Sorouraddin and A. M. Haji. 1998. Determination of mercury by cold vapour atomic absorption spectrometry after preconcentration with dithizone immobilized on surfactant-coated alumina. J. Anal. At. Spectrom. 13: 305-8.

Passos, C.J., D. Mergler, E. Gaspar, S. Morais, M. Lucotte, F. Larribe, R. Davidson and S. de Grosbois. 2003. Eating tropical fruit reduces mercury exposure from fish consumption in the Brazilian Amazon. Environ. Res. 93: 123-130.

Rados, C. 2004. EPA Revise Guidelines on Mercury in Fish. FDA Consumer Magazine. 29:3 http://www.cfsan.fda.gov/~dms/admehg3.html (accessed November 16, 2005).

Ren, J.M., M. E. Rybak and E. D. Salin. 2003. Elimination of arcing in induction heating-electrothermal vaporization (IH-ETV) for sample introduction into inductively coupled plasmas. J. Anal. At. Spectrom. 18: 485-486.

Rybak, M.E. and E. D. Salin. 2001. Direct Determination of Metals in Soils and Sediments by Induction Heating-Electrothermal Vaporization (IH-ETV) Inductively Coupled Plasma-Optical Emission Spectrometry (ICP-OES). Appl. Spectrosc 55: 816-821.

Rybak, M.E. and E.D. Salin. 2001. Development and characterization of induction heating-electrothermal vaporization (IH-ETV) sample introduction for inductively coupled plasma spectrometry. Spectrochim. Acta, Part B 56B: 289-307.

Salin, E.D. and J. M. Ren. 2003. Direct filter vaporization with induction heating-electrothermal vaporization (IH-ETV) and a foam carbon surface. J. Anal. At. Spectrom. 18: 953-954.

Skoog, D.A, D.M. West and F.J. Holler. 1996. Fundamentals of Analytical Chemistry. 7th ed. New York: Saunders College Publishing, 630.

SIemr, F., W. Seiler, C. Eberling, and P. Roggendorf. 1979. The Determination of Total Gaseous Mercury in Air at Background Levels. Analytica Chimica Acta, 110: 35-47.

Takaya, M. and N. Kohyama. 2004. An improved gold amalgam method for measurement of mercury vapor in the workplace. Journal of Occupational and Environmental Hygiene, 1: D75-D79.

Toribara, T.Y. and D. A. Jackson. 1982. Nondestructive x-ray fluorescence spectrometry for determination of trace elements along a single strand of hair. Anal. Chem. 54: 1844-1849.

Valkovic, V., D. Miljanic, R. M. Wheeler, R. B. Liebert, T. Zabel and G. C. Phillips. 1973. Variation in trace metal concentrations along single hairs as measured by proton-induced x-ray emission photometry. Nature 111: 251-252.

The Mystery of Rhomboid in Capicua mutant Fruit Flies

Ali Saleem Hassan, Laura A. Nilson – Supervisor

Department of Biology, McGill University, Montreal, H3A 1B1, Quebec, Canada

Introduction

Drosophila melanogaster is a fruit fly that is one of the most commonly used animal model for genetic studies. Dorsal-ventral (dv) patterning, which is the body plan, of the Drosophila embryo is determined by the asymmetric positioning of different underlying cellular molecules. DV patterning of the Drosophila embryo is established well before fertilisation. The Drosophila egg develop within a cluster of cells consisting of an oocyte interconnected with fifteen sister nurse cells, which function as a source of RNAs and proteins for the developing oocyte and degenerate by the end of oogenesis. Surrounding this cluster is an epithelium of follicle cells, which provide yolk and secrete the eggshell (Fig1). Initial dv asymmetry is established at mid oogenesis and the information is then passed on to the surrounding follicle cells (3). The protein gurken (grk), in the oocyte, provides the initial polarizing signal to initiate the formation of the eventual polarity of the egg, and activates Drosophila epidermal growth factor receptor (EGFR) signaling in the dorsal follicle cells. Through positive and negative feedback mechanisms, this EGF signaling is refined and defines a precise pattern of cell fates within the follicular epithelium (3). This specific definition of fates will be used as a basis to understand the effects of the gene capicua (cic) on follicle cell fate patterning.

Key Terms

Follicle:
a small bodily cavity or sac, such as the oocyte.

Oogenesis :
the stages of development and maturation of the female reproductive gamete

Ectopic:
an abnormal location or position

Mapping Crosses:
Mating crosses designed to locate the chromosomal position of a given gene.

Mosaic Flies:
Flies that carry a mixture of mutant and wild-type cells

Cell Autonomous:
Expression in a given cell independent of other cells

RNA Probes:
Strands of RNA that are complementary to the RNA of study.

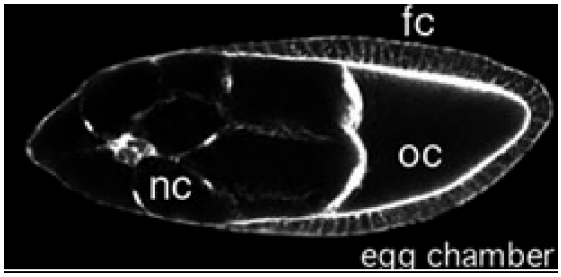

Figure 1. Drosophila egg chamber. The developing oocyte cell (oc) is interconnected with 15 nurse cells (nc). Surrounding these cells is an epithelium of follicle cells (fc)

Expression of rho in cic mutant ovaries

Follicle cells generate an eggshell embellished with external structures including the long respiratory appendages located dorsally at the anterior of the egg (Fig 2). Since external structures reflect the follicular patterning along the dv axis of the mature egg, any defect in the patterning will be reflected by anomalies in the resulting eggshell. Females lacking cic function lay eggs that display an expansion of the dorsal features to the ventral half of the egg. This phenotype, most prominently, includes broad dorsal appendages that are laterally shifted and a collar of ectopic dorsal appendage material near the ventral anterior circumference of the maturing oocyte (Fig 3, right panel). Typically this eggshell phenotype is linked to EGFR activation and of its subsequent target genes including mirror (mirr), kekkon 1 (kek1), and rhomboid (rho) (1). However in cic mutant ovaries analysis of mirr and kek 1 expression patterns reveals that mirr expression expands ectopically in the follicular epithelium leading to a dorsalized phenotype, but the expression of kek 1 remains unaffected (2) (Fig 2). This indicates that cic plays a role in regulating the expression of mirr but not that of kek 1, and that mirr is under the control of cic.

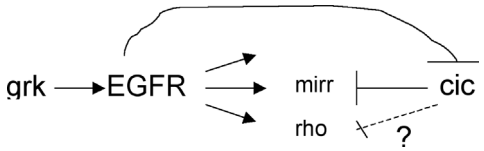

Figure 2. The above pathway is not absolute and only represents the important players for this study. grk protein in the oocyte activates the epidermal growth factor receptor (EGFR) which then goes on to activate kek 1, mirr, rho and inactivate suppress expression of cic in the dorsal half of the Drosophila egg. Manipulation of this expression allowing it to expand to the ventral half of the embryo will lead to a dorsalised embryo. Females mutant for the gene cic lay dorsalised embryos where the expression of mirr was expanded but not that of kek 1.

Interestingly, ectopic expression of rho in flies generates dorsalized eggs, with the characteristic broadened and laterally shifted dorsal appendages similar to those seen in cic mutant flies (1). One would then hypothesize that rho is also under the control of cic just like mirr.

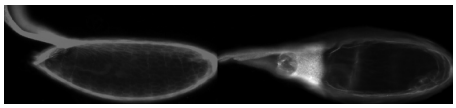

Figure 3. Wildtype (WT) egg (left) versus cic mutant egg (right). Notice the difference in shape of the egg and the dorsal appendages between WT and cic.

Materials and Methods

To test the above prediction, a Fluorescent In Situ Hybridisation (FISH) was performed to visualise rho mRNA expression in both cic mutant ovaries, and wildtype controls for comparison. FISH involves the use of RNA probes that are complementary to the mRNA in question. The RNA probes bind to the complementary mRNA in the tissue and with the use of fluorescent antibodies against the RNA probe one can visualise the location of the particular mRNA.

Moreover, the difference in appendage fate in cic mutant ovaries was investigated. Since cic mutant flies generate eggs that exhibit abnormal dorsal appendages, it can be concluded that cic is involved in defining the two populations of cells that make up the dorsal appendages. The transcription factor Broad-Complex (BR-C), expressed by the roof cell population, which go on to make the actual appendage, has been used as a visual marker to study the fate of these cells on a cic mutant background. Results have shown that BR-C expression expands to the ventral half of the follicular epithelium in ovaries lacking cic, forming a collar around the anterior-most circumference of the maturing oocyte (1). The roof cells make up only part of the dorsal appendages, and thus tell only part of the story. Thus, rhomboid-lacZ (rho-lacZ) was used to visualize changes in the floor cell fate patterning, which go on to make up the base of the appendages.

Results

The FISH technique worked against grk mRNA (positive control for technique) in wildtype ovaries (Fig 3). Unfortunately, similar results failed to be reproduced with the grk mRNA probes and the rho mRNA probes built for the purpose of this experiment. Troubleshooting the probes will be performed to determine the proper functioning of the technique.

Furthermore, the chromosomal position of the rho-lacZ transgene, which is an artificially inserted gene, in the Drosophila stock came into question. After resolving this issue through conducting mapping crosses, it will be possible to use the transgene as a reporter to visualize changes in floor cell fate patterning. Additionally, mosaic flies bearing clones of cic mutant follicle cells will be generated genetically to further characterize the expression of rho-lacZ. It will also be determined whether changes in the expression of rho-lacZ are cell autonomous. Lastly, the above experiments will be complemented by testing for the suppression of the cic mutant phenotype through reduction of the expression of rho and/or mirr, and in time by characterizing how cic regulates rho and/or mirr. This analysis of rho in a cic mutant background will further our understanding of the important pathway that regulates dv patterning of the Drosophila egg, and advance Drosophila developmental research a small step, with the final goal being application of this research to humans.

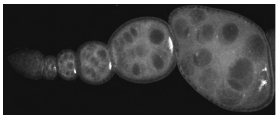

Figure 4. Grk mRNA FISH of single ovariole of a wildtype female ovary. The ovariole is like an assembly line with every subsequent egg chamber at a later stage of oogenesis than the egg chamber before it. The grk mRNA fluoresces red here and is seen localising near the maturing oocyte nucleus.

References

1. Atkey, M.R., Lachance, J.B., Walczak, M., Nilson, L. A. (Submitted). Capicua regulates follicle cell fate in the Drosophila ovary through repression of mirror

2. Goff, D.J., Nilson, L.A., Morisato D. (2001). Establishment of dorsal-ventral polarity of the Drosophila egg requires capicua action in ovarian follicle cells. Development **128, 4553-456**

3. Nilson, L.A., Schupbach, T., (1999) EGF receptor signalling in Drosophila oogenesis. Curr Top Dev Biol. **44, 203-43**

The Vestibular Ocular Reflex In Parkinsonian Mice

Irene Raitman and Kathleen E. Cullen

Department of Physiology, McGill University, 3655 Sir William Osler Dr., Montreal, Quebec, Canada, H3G 1Y6.
Correspondence should be addressed to Irene Raitman: irene.raitman@mail.mcgill.ca

Introduction

Parkinson's disease (PD) is a progressive neurological disorder characterized by poor balance, slow movement, rigidity, and uncontrollable tremors of the hands. These symptoms result from the degeneration of dopamine-producing nerve cells in the brain, specifically in the substantia nigra and the locus coeruleus. Dopamine is a neurotransmitter that is released by the brain and stimulates motor neurons. When dopamine production is depleted, the motor system is unable to control movement and coordination and PD symptoms occur.

The goal of this experiment was to gain a better understanding of the effects of PD on the vestibular system. More specifically, the effect of the destruction of the dopamine producing cells on the vestibular ocular reflex (VOR) was investigated. The VOR is a gaze-stabilization reflex which maintains eye fixation on an object during head rotation. As the head turns, the eyes compensate by slowly turning in the opposite direction. As the eyes reach the limit of their turning range, they quickly reset by returning to their starting position. Together, the VOR (slow phase) and the resetting (quick phase) make up the vestibular nystagmus. The VOR produced during horizontal and vertical rotations by untreated mice was compared with the VOR produced by those mice that were injected with MPTP (1-methyl-4-phenyl-1,2,3, 6-tetrahydropyridine), a drug known to destroy the dopamine producing neurons in humans, primates, and rodents. In addition, the relationship between peak eye velocity and amplitude of the quick phases was analyzed to see if the quick phase was altered in MPTP-treated mice.

Methods

Prior to injection, eye movement recordings from two-month-old male mice were used to establish a VOR baseline. These mice were then injected with MPTP for a period of five days. Seven days after the start of the injection treatment, recordings were taken from the mice to determine the changes in the VOR and quick phase. Horizontal VOR was recorded at 20 and 40 deg/s rotations at frequencies from 0.1 Hz to 1.6 Hz. These velocities and frequencies were chosen because they are commonly used in the literature for VOR recordings. Vertical VOR was recorded at the same frequencies as the horizontal VOR, but only at 20 deg/s due to experimental constraints. Recordings for both the untreated and MPTP-treated mice were done in both light and dark conditions. The dark condition allowed for a more accurate measurement of the VOR to be taken because it eliminated visual cues that might have enhanced the VOR. An infrared pupil tracker video system was used to record the eye movements. Gain was then calculated from the eye movement data. Gain is eye velocity divided by head velocity. Under normal circumstances, the value for gain tends to be close to 1 due to the ability of the eye to closely compensate for head rotation by turning in the opposite direction. The mice were head-fixed to make the head velocity equal to the velocity of the turntable to which the mice were fixed. For analytical purposes, the gains of the MPTP-treated mice were normalized to the gains of the untreated mice. This was accomplished by setting the mean gains of the untreated mice to 1 for all frequencies and velocities. The MPTP gains were then altered by the corresponding amounts.

Results and Discussion

The horizontal eye position/head position traces of untreated mice were compared to the traces of MPTP-treated mice. The amplitudes of the eye position signals were lower in the MPTP-treated mice, therefore, the VOR gains were lower in these mice (Fig.1). When the MPTP-treated mouse data was normalized to the untreated mouse data, it was observed that in both light and dark conditions that the horizontal gains were significantly lower than 1 (Fig. 2 and 3). At the higher rotation velocity, the gains slightly increased but were still lower than 1. In light conditions, the largest reduction in VOR gain from normal values occurred at 0.4 Hz. These normalized gains were 0.42 and 0.53 at 20 and 40 deg/s rotations respectively (Fig. 2).In dark conditions, for frequencies less than 1 Hz, the gains were similar to those in light conditions. However, at 1.6 Hz, the gains were reduced more than they were at the same frequency in light. More specifically, at a velocity of 20 deg/s, the largest reduction in gain occurred at 0.4 Hz with a value of 0.47, while at a velocity of 40 deg/s it occurred at 1.6 Hz with a value of 0.48 (Fig. 3).

In contrast to the horizontal VOR results above, the normalized vertical VOR gains of MPTP-treated mice showed relatively little reduction. The vertical gains were greater than 0.6 across all frequencies tested for both light and dark conditions (Fig. 4 and 5). The lowest gain observed in light conditions was 0.68 at 0.8 Hz (Fig. 4). In dark conditions, it was seen that at the higher frequencies of rotation, the gains were slightly less than those in the light, with the lowest gain being 0.59 at 1.6 Hz (Fig. 5).

In addition, the relationship between the peak velocity of the quick phases and their associated amplitudes was not altered in MPTP-treated mice. The results were comparable to those found in the untreated mice. This finding is similar to those that have been found in human PD subjects (Hotson et al. 1986; Rottach et al. 1996).

These results show that MPTP-treated mice have subnormal VOR gains, with horizontal VOR being more affected than vertical VOR. This suggests a role for dopamine in the proper execution of the VOR. However, because the quick phases were not affected, it appears that dopamine depletion does not affect the brainstem neurons responsible for the quick phase. Hence MPTP only targets the VOR pathway and not the brainstem pathway that controls the quick phase. However, it remains to be determined where in the VOR pathway dopamine, and therefore MPTP, acts.

Example of the Horizontal VOR in the Dark for an Untreated and a MPTP-treated Mouse

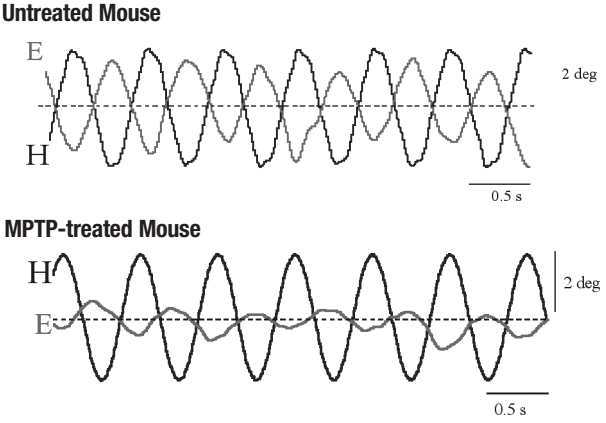

Figure 1. Untreated and MPTP-treated Horizontal VOR Traces: Horizontal VOR in the dark for untreated mouse 5E (left) and MPTP-treated mouse 6F (right) showing the head position (H) and the sinusoidal eye position (E). The mice were rotated at 20 deg/s velocity at 1.6 Hz. (Data presented is representative of all data)

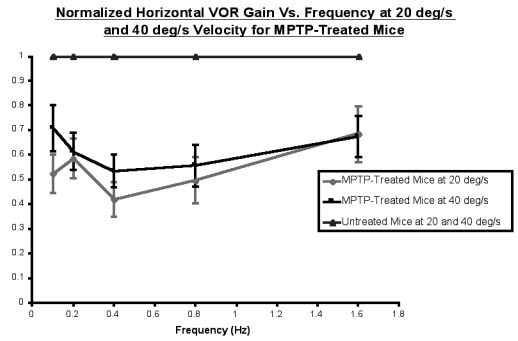

Figure 2. Normalized MPTP-treated Horizontal VOR in the Light Gains: Mean normalized gains from five MPTP-treated mice rotated horizontally at both 20 and 40 deg/s velocities. Untreated mice gains have been normalized by setting all gains to 1. Error bars represent SEM.

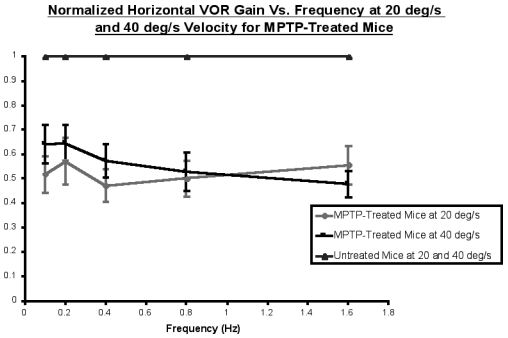

Figure 3. Normalized MPTP-treated Horizontal VOR in the Dark Gains: Mean normalized gains from five MPTP-treated mice rotated horizontally at both 20 and 40 deg/s velocities. Untreated mice gains have been normalized by setting all gains to 1. Error bars represent SEM.

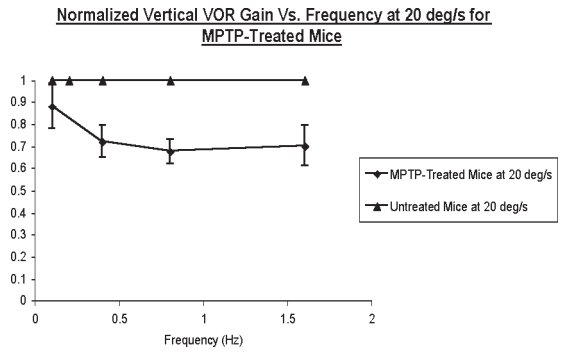

Figure 4. Normalized MPTP-treated Vertical VOR in the Light Gains: Mean normalized gains from five MPTP-treated mice rotated vertically at 20 deg/s velocity. Untreated mice gains have been normalized by setting all gains to 1. Error bars represent SEM.

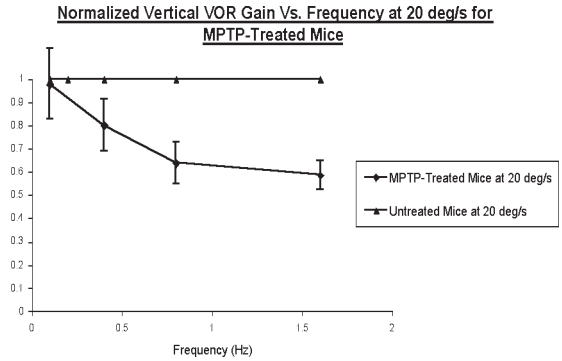

Figure 5. Normalized MPTP-treated Vertical VOR in the Dark Gains: Mean normalized gains from five MPTP-treated mice rotated vertically at 20 deg/s velocity. Untreated mice gains have been normalized by setting all gains to 1. Error bars represent SEM.

Conclusion

Gaze stabilization reflexes in MPTP-treated mice can not compensate for the loss of dopamine producing neurons completely. This suggests that dopamine is needed for a proper VOR. This serves as supporting evidence for MPTP-treated mice as a PD model. Now that a link has been discovered between dopamine and the VOR, further studies are needed to determine where dopamine acts in the VOR pathway. Future experiments should look at both vestibular and visual pathways to see if they are affected by dopamine depletion. Hopefully, the knowledge gained from these mice models about PD will eventually lead to new treatments for this debilitating disease.

References

1. Hotson JR, Langston EB, Langston JW. Saccade responses to dopamine in human MPTP induced parkinsonism. Annals of Neurology. 1986 Oct; 20(4): **456-63**.

2. Rottach KG, Riley DE, DiScenna AO, Zivotofsky AZ, Leigh RJ. Dynamic properties of horizontal and vertical eye movements in parkinsonian syndromes. Annals of Neurology. 1996 Mar; 39(3): **368-77**.

3. Stahl JS, Van Alphen AM, De Zeeuw CI. A comparison of video and magnetic search coil recordings of mouse eye movements. Neuroscience Methods. 2000; 99(1-2): **101-10**.

Molecular Mechanisms Controlling the Differentiation of Germ Cells in mammals: Divergent expression patterns of SLBP in male and female meiotic cells and their developmental consequences.

*Kyle J. Martin and Hugh J. Clarke**

Department of Biology, McGill University, 1205 Avenue du Docteur Penfield, Montréal, Québec, Canada H3A1B1.
Correspondence – hugh.clarke@muhc.mcgill.ca

Abstract

The stem-loop binding protein (SLBP) binds to replication-dependent histone mRNA and participates in its processing, stabilization and translation. It has previously been shown that SLBP expression in somatic cells is regulated by the cell cycle. Our work demonstrates that male and female germ line cell expression patterns differ dramatically both from the somatic cell-cycle regulated pattern, and from each other. Using immunofluorescence on a post-natal series of male and female gonads, SLBP was shown to translocate from the cytoplasm of non-growing oocytes to the nucleus upon initiation of growth, followed by re-entry into the cytoplasm upon entry into metaphase II. In contrast, developing male germ cells initially express SLBP at high levels both in the nucleus and the cytoplasm, followed by cytoplasmic segregation and finally complete absence of expression by maturation. We believe that these divergent expression patterns in male and female germ cells reflect the different requirements for SLBP in cell differentiation and early embryogenesis, respectively.

Introduction

Understanding how a complex organism results from a single cell is the focus of research in developmental biology, and despite the identification of numerous pathways and processes involved, it remains one of the most persistent and intriguing questions in current biology. A few hundred years ago the prevailing theory for development, known as preformation, was that miniaturized copies of adults existed ready-made inside the egg. In modern times, we have come to view development as a process of epigenesis: the progressive addition and differentiation of characters beginning from an undifferentiated state – ultimately, the fertilized egg. Molecular, genetic, and embryological approaches have all been used to gain a better appreciation of this process, but there remains an overwhelming amount of work to be done, even with model systems such as the mouse.

Without the precisely orchestrated process of germ cell specification and maturation, embryogenesis would not occur normally. It therefore stands to reason that in order to fully comprehend animal development, both the haploid (germ cell) and diploid (embryonic; adult) stages of the life cycle must be considered. The molecular mechanisms controlling germ cell development, and their relationship to embryonic development, are active areas of research.

Eukaryotic DNA is packaged as chromatin, a structure consisting of DNA bound to proteins known as histones. In order for cell division to take place, not only must DNA be duplicated, but a sufficient supply of new proteins for DNA packaging must also be available. The stem-loop binding protein (SLBP) is a 31kDa RNA-binding protein that binds to a conserved stem-loop sequence in the 3'-untranslated region of histone mRNA and plays a key role in cellular proliferation by promoting the expression of histones. In somatic cells, most histones are synthesized during S-phase, the stage of the cell cycle where DNA is replicated. SLBP accumulates just prior to the onset of S-phase, and following S-phase, it is rapidly degraded [Whitfield et al. 2000; Marzluff and Duronio 2002].

Results

In order to define the role of SLBP in meiotic cells, we used immunofluorescence on sectioned ovarian tissue to detect its expression in the developing oocyte. We found that SLBP is present only the cytoplasm of non-growing oocytes and that upon initiation of oocyte growth, SLBP accumulates to very high levels in the nucleus (figure 1). It remains sequestered in the nucleus during the stage when it would normally be degraded in somatic cells. Only upon progression to metaphase II does SLBP relocate to the cytoplasm where it participates in the translation of histone messages [Allard et al. 2002; our data].

To assess whether SLBP had a conserved role in meiotic cells, we examined the expression of SLBP in developing spermatozoa using immunofluorescence on sectioned testes. Strikingly, the expression pattern was nearly the converse of that seen in oocytes, and markedly different from somatic cells. Early in male meiotic cell development, spermatogonia and spermatocytes expressed SLBP at high levels in both the nucleus and the cytoplasm. Later in development, SLBP becomes sequestered to the cytoplasm in a subset of the spermatocyte population, before its expression is lost completely by the spermatid and spermatozoa (mature sperm cell) stage (figure 2). These results were verified by immunoblotting protein extracts from isolated male germ cell populations, which showed a progressive loss of SLBP as cell populations matured (data not shown).

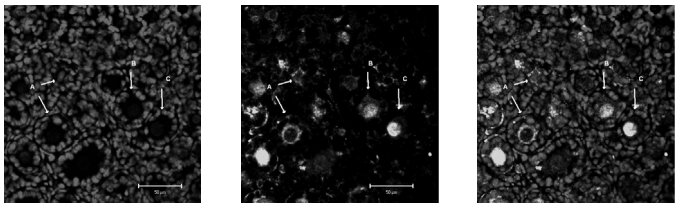

(1) DNA stain (PI) (II) SLBP (488-tyramide) (III) DNA/SLBP overlay

Figure 1. Three-day old ovarian section Cytoplasmic SLBP (A) present in the oocytes in primordial non-growing and early growing follicles. A rapid transition from the cytoplasm to the nucleus appears to occur as SLBP begins to accumulate in the nucleus (B) while some remains cytoplasmic, and finally becomes nearly entirely nuclear (C).

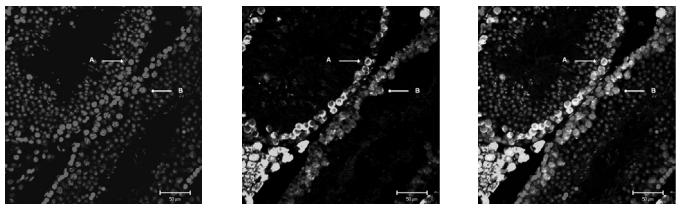

(1) DNA stain (PI) (II) SLBP (488-tyramide) (III) DNA/SLBP overlay

Figure 2. Seven-week old testis section SLBP is present exclusively in a subset of the developing male germ line population. SLBP is localized either exclusively in the cytoplasm (A) or is present both in the cytoplasm and the nucleus (B) according to the stage of development of the germ cells. As the male germ cell develops SLBP is lost.

Discussion

Unlike a somatic cell, the mammalian oocyte must accumulate massive amounts of protein and mRNA necessary for not only one, but several cell divisions in the early stages of embryonic development [Song and Wessel 2005]. We believe that the high level of SLBP in the cytoplasm, followed by its translocation and concentration in the nucleus is necessary in order to safe-guard the histone messages until they are needed, which is upon fertilization. In support of this interpretation, mutant mice expressing RNAi targeted against SLBP, specifically in the growing oocyte, yield embryos whose development arrests at the 2-cell stage [H. Clarke, unpubl. data]. This presumably owes to a deficit of histones, which impedes the ability of the blastomeres to divide beyond the 2-cell stage. Prior to fertilization, the oocyte does not replicate its DNA, and high histone and SLBP levels do not seem to be necessary for oocyte survival, as embryos are able to reach the 2-cell stage. It therefore seems that the reason for the high level of SLBP expression in the oocyte is to facilitate development of the embryo.

The developing male germ cell does not accumulate histones to constitute early embryonic chromatin. In fact, during the process of maturation, the spermatozoa even ultimately replace their own histones with protamines, proteins more efficient at condensing the DNA into a tiny streamlined capsule for efficient transport to the egg [Govin et al. 2004]. Early in this process of chromatin remodeling, however, several histone variants are first synthesized and loaded onto the chromatin. We suggest that the high levels of SLBP expression seen in both the nucleus and cytoplasm during the early stages of spermatogenesis, before the bulk remodeling takes place, is due to the stockpiling of histone variants for this process. Later in development, the attenuation of SLBP may be necessary in order to deplete histone expression and facilitate replacement by the more effective DNA condensing proteins. Experiments are currently being planned to test this hypothesis. Transgenic mice over-expressing SLBP in maturing spermatozoa will be assayed for functional defects in the remodeling process. Because this remodeling process is undone by the oocyte upon fertilization using the stockpile of histones, and no function for highly condensed male chromatin has yet been found for embryonic development, the best way to account for SLBP expression pattern in the male germ line is that it is required for the differentiation of sperm cells. In other words, germ line developmental demands

govern SLBP expression patterns in spermatozoa, as opposed to embryonic development, for which SLBP is required in the oocyte.

Methods

Histology

Ovaries and testes were dissected from CD-1 mice and fixed overnight in a 10% formalin solution at 4°C with agitation. Tissue was dehydrated through a graded ethanol/xylene series, embedded in paraffin, and stored at -20°C until needed. 5_m sections were cut on a microtome and mounted on slides, and stored at 4°C for up to 24 hrs. Rehydration was followed by antigen recovery in 0.1% sodium citrate at 80-90°C for 15min.

Immunofluorescence

Slides were blocked in 0.1% tween-20, 5% BSA, 5% goat serum for 30 min, and then incubated in purified anti-SLBP 1:200 in block overnight at 4°C. Slides were washed in PBS, and then incubated with HRP conjugated secondary antibody diluted 1:200 in block for 1hr at room temperature. Slides were then incubated with Alexa Fluor 488-labeled tyramide for 10 min. Slides were washed, and propidium iodide diluted to 0.1ng/_l was added for 5 min. Slides were mounted in mowiol and stored dark at 4°C. Images were captured using a confocal microscope.

References

1. Allard, P., Champigny, M. J., Skoggard, S., Erkmann, J. A., Whitfield, M. L., Marzluff, W.F., and Clarke, H. J. (2002). Stem-loop binding protein accumulates during oocyte maturation and is not cell-cycle-regulated in the early mouse embryo. Journal of Cell Science. **115, 4577-4586.**

2. Govin, J., Caron, C., Lestrat, C., Rousseaux, S., and Khochbin, S. (2004). The role of histones in chromatin remodelling during mammalian spermiogenesis. Eur. J. Biochem. **271, 3459-3469**

3. Marzluff, W. F., and Duronio, R. J. (2002). Histone mRNA expression: multiple levels of cell cycle regulation and important developmental consequences. Current Opinion in Cell Biology. **14: 692-699**.

4. Song, J. L., and Wessel, G. M. (2005). How to make an egg: transcriptional regulation in oocytes. Differentiation. 73:**1-17**.

5. Whitfield, M. L., Zheng, L.-X., Baldwin, A., Ohta, T., Hurt, M. M., and Marzluff, W. F. (2000). Stem-Loop Binding Protein, the Protein That Binds the 3' End of Histone mRNA, Is Cell Cycle Regulated by Both Translational and Posttranslational Mechanisms. Molecular and Cellular Biology. 12: **4188-4198**.

Photograph by Claudio Callagaris

The Difficulty In Computing Ancestral DNA Sequences: Using Computational Analysis To Reconstruct DNA Sequences

Zhentao Li[a] and Mathieu Blanchette[b]

[a]School of Computer Science, McGill University, 3480 University St., Montreal, Quebec, Canada, H3A 2A7.
[b]McGill Centre for Bioinformatics, 3775 University St., Rm. 332, Montreal, Quebec, Canda, H3A 2B4.
Correspondence should be addressed to Zhentao Li: zhentao.li@mail.mcgill.ca

Intriguing work has been carried out in order to decipher the genetic codes of today's existing species. However, little is known about the genetic makeup of species that existed long ago. Exciting possibilities have recently been raised in the field of computational analysis (1), proposing that reconstruction of ancestral DNA sequences can be performed if the DNA sequences of the existing species are known. Being able to perform such reconstructions would simplify the study of the evolution of these species, and uncover many mysteries regarding life that once existed on this planet.

In order to perform reconstructions of unknown ancestral DNA sequences, many different types of problems must be solved, all of which can be approached computationally. Examples of such problems include building a phylogenetic tree of the evolutionary line in question, determining a multiple alignment of the existing species being analyzed, or working out the actual identity of the nucleotides within the ancestral sequence. The problem presented in this paper considers the level of modification within the ancestral sequence.

Key Terms

Phylogenetic tree:
a tree-like diagram demonstrating the relationship between ancestral species and contemporary species

Multiple alignment:
an alignment of DNA sequences, whereby homologous positions are lined up with respect to one another

Deletion:
takes all characters (0 or 1) in a contiguous region, and transforms them into 0's (gaps). For example, '10101' becomes '00000'

Insertion:
takes a contiguous region of 0's (gaps) and transforms some of the 0's into 1's (nucleotides). For example, '00000' becomes '10101'

Instance:
a specific case or an occurrence of a problem. For example '3 +4 = ?' is an instance of the addition problem 'a+b=?'

Problem reduction:
turning all instances of one problem into instances of another problem

Reducing:
showing that a problem can be solved by using the solution to another problem

Considering the diversity of the problems at hand, one must realize that not all of these computational problems can be solved. In other words, the complexity of certain problems is such that it would currently take a computer an unrealistic amount of time to solve these types of problems. In such situations, these problems are deemed 'hard'.

The following analysis will provide a detailed computational definition of the problem in question. The aim is to define the components of the analyzed problem, and will not provide any solution to the problem. This definition is succeeded by the problem reduction, which will assess the hardness of the problem at hand. In fact, it will be shown that the problem is 'hard', and is impractical to solve. This is achieved by reducing a standard computational problem known to be hard to the problem in question.

Problem Definition

In order to attempt to solve the problem in question, input data are necessary, which include the sequences of the existing species, the phylogenetic tree for this evolutionary line, and the multiple alignment of the present-day species' sequences (fig. 1, a-c). The phylogenetic tree is necessary to give an idea of how the species are related to one another. Existing species occupy the outside positions of the tree, termed the 'leaves', while the ancestral species occupy the internal positions of the tree, termed the 'nodes' (fig. 1, a). The multiple alignment is used to analyze a specific stretch of DNA within each species being analyzed and to compare the differences and similarities between the stretches. Once

aligned, the sequences are then transformed into an arbitrary code of 1's and 0's, based on the presence or the absence of a nucleotide at each position (fig. 1, d). If a nucleotide exists at a certain position, it is transformed into a 1. Conversely, if no nucleotide (i.e. a gap) exists at a certain position, it is transformed into a 0. The task is then to find the most probable sequences of 0's and 1's at the internal nodes, which represent the sequences of the ancestral species. Such a set of sequences is called a solution. In this model, the most probable sets of sequences are those that will minimize the total number of sequence changes in the tree. A change can manifest itself as either a deletion or an insertion. There is an extra restriction, which is that a previously deleted nucleotide within the timeline cannot be re-inserted at a later time into a specific sequence within the tree. A solution which minimizes the number of insertions and deletions is called an optimal solution. An example of a solution is shown in fig. 2.

Problem Reduction

Now that an example of the problem has been shown, the problem reduction will prove that it cannot realistically be solved. In other words, this problem is deemed 'hard'. As such, there is no general way of finding a solution to the type of problem described previously in the problem definition. Consider the problem in question to be named ADR, for 'ancestral DNA reconstruction'. The way in which this problem is shown to be hard is by proving that it is at least as difficult to solve as a "benchmark" problem, named NAE-3SAT. NAE-3SAT, or 'not all equal 3 satisfiability', is a problem that is known to be computationally difficult in the field of computer science. The way in which this is proven is to show that any instance of NAE-3SAT can be reduced to ADR.

NAE-3SAT Problem Definition

An instance of the NAE-3SAT problem consists of variables, literals and clauses. The variables (named X1, X2, etc) can be assigned a value of either 'true' or 'false'. A literal is either a variable (e.g.:X3) or the negation of a variable (e.g.:$\bar{X}$1). A clause is a set of three literals.

In an NAE-3SAT problem, the goal is to assign a value (true or false) to each of the variables that satisfy all the clauses in the problem. A clause is satisfied if at least one literal is assigned as 'true' and at least one literal is assigned as 'false'. For a given assignment of the variables, the literal Xi is assigned the same value as the variable Xi and the literal $\bar{X}$i is assigned the opposite value. An assignment which satisfies all the clauses is called a satisfying assignment. A solution to an instance of NAE-3SAT is a satisfying assignment.

The proof

The following is a simplified version of the proof. This is the general scheme used to reduce a problem.

Assume that there is a way to solve ADR, without performing an unrealistically large amount of computations. NAE-3SAT can then be solved computationally in the following manner:

1. Given an instance of an NAE-3SAT problem, construct an appropriately chosen instance of ADR. In other words, determine the input that one wishes to analyze.
2. Solve this instance of ADR, which consists of inputting the data that was determined in (1). This is possible, as it was previously assumed that there was a way of solving ADR.
3. Obtain the solution that is found for the ADR problem and translate it into a solution to NAE-3SAT.

If it is determined that ADR can be solved once these computational analyses have been performed, then NAE-3SAT can also be solved. This would contradict the hardness of NAE-3SAT. Therefore, the initial assumption that we could solve ADR quickly must have been false. The whole proof now relies on constructing the so-called 'appropriate chosen instance' of ADR given an instance of NAE-3SAT. The rest of the proof is a description and explanation of this construction. Recall that a phylogenetic tree must be given in an instance of ADR. In this construction, it will have the shape shown in fig. 2, b.

If there is a satisfying assignment to the given instance of NAE-3SAT, it must somehow be found. In this construction, this shall be obtained from the sequence found at the S node of the phylogenetic tree shown in fig. 3, b. On the other hand, if there is no satisfying assignment to the instance of NAE-3SAT, the construction will force the total number of operations (i.e. insertions or deletions) in any optimal solution to be greater than some fixed number.

In preparation for step 3, any optimal solution for the sequence in the S node will be forced to have a certain

structure, allowing it to be translated in such a way that it becomes a solution to NAE-3SAT.

Initially, some of the positions of the sequence within the S node are forced to be 1 in any optimal solution. This is done by setting some of the leaves to specific strings. In so doing, other solutions will be forced to have more operations. This will be useful since if both the sequences within the S node and within a given leaf have a 1 at any given position, no insertion or deletion can go through this position (recall that a nucleotide cannot be re-inserted once deleted).

A region of contiguous positions in the S node will be reserved for each variable in this particular instance of NAE-3SAT. Depending on what is in this region of the S node sequence, one will know what to assign the variables in the NAE-3SAT problem (if a satisfying assignment exists). In fact, the idea is to force each region to only have two possible values in any optimal solution. Again, this is achieved by forcing other solutions to have more operations. Depending on which of the two values is assigned, it will become clear as to what value (true or false) is to be assigned to each variable.

The only remaining task is to ensure that the solution obtained will satisfy each clause. A different set of leaves can be used for each clause. Such a task is not as simple as it first seems. However, one easy aspect of this operation is to construct leaves in which the number of literals in a clause assigned 'true' can be counted. In this particular sense, the term counted refers to the fact that the number of operations needed is proportional to the number of literals set to true. But more than just counting is needed.

It is necessary to force any optimal solution to have at least one literal set to true and at least one literal set to false in any clause, if there is indeed a satisfying assignment. To do so, strings are designed at the leaves which can count the number of literals set to true, two at a time. Along with other such tricks, like taking combinations of different strings, this will guarantee to find a satisfying assignment, if it exists.

Conclusion

The most immediate implication of the hardness of the ADR problem is that large instances of the problem (ex.: 1,000,000 nucleotides) are most likely not going to be solved in a rapid manner. This is problematic in practice as the large problems, such as reconstructing whole genes, are those that generate the most interest. However, the findings described above do not render this reconstruction hopeless, as other smaller instances of the problem may still be solved. It would also be possible to obtain sub-optimal solutions for these larger instances, though accuracy would be lost in such a reconstruction. Though many obstacles remain towards achieving the goal of ancestral genome reconstruction, computational analysis is still a powerful tool by which such reconstructions can be performed.

Special thanks to Leonid Chindelevitch for his contributions to this project.

References

1. Mathieu Blanchette, Eric D. Green, Webb Miller, and David Haussler. Reconstructing large regions of an ancestral mammalian genome in silico. Genome Res., 14(12):**2412-2423**, December 2004.

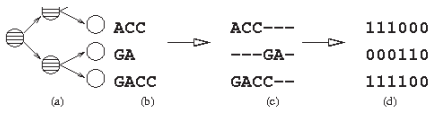

Figure 1. Example of information input. Clear circles represent the existing species, termed the leaves of the tree. Dashed circles represent the ancestral species, termed the internal nodes of the tree. (a) A phylogenetic tree. (b) DNA sequences of the existing species. (c) Multiple alignment for sequences found in (b). A '-' represents a gap. (d) Conversion of the nucleotide input into an arbitrary code of 1's and 0's.

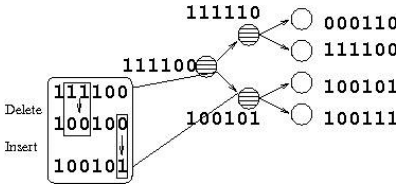

Figure 2. Example of a solution. The highlighted branch, denoted by a box, shows an insertion and a deletion.

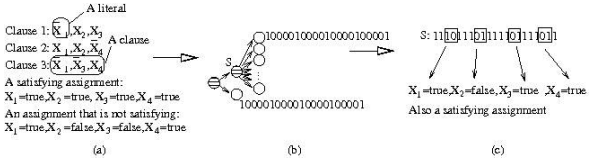

Figure 3. (a) Example of an instance of NAE-3SAT along with a satisfying assignment. The second assignment is not satisfying since all literals within clause 1 are set to false. (b) An instance of ADR is constructed and then solved. (c) The solution is analyzed, looking specifically at the string within the S .node. From this, a satisfying assignment for NAE-3SAT can be found

Successional Dynamics in Seagrass Communities

Charalampos Mavromatis, Sandra Binning, Frédéric Guichard*

Department of Biology, McGill University, 1205 Avenue du Docteur Penfield, Montreal, Quebec, Canada H3A1B1. (514) 398-4117
** Correspondence should be addressed to charalampos.mavromatis@mcgill.ca*

Abstract

The sequence of ecological changes in which one species is replaced by another is known as succession. Den Hartog (1971) was the first to propose successional schemes for seagrass communities based on competition-colonization hierarchies, which have rarely been challenged. Wave-disturbed subtidal systems are characterized by the presence of gaps, the distinct topographic depressions devoid of vegetation defined. We present a study of a Caribbean seagrass bed exemplifying macroalgal-seagrass succession dynamics in relation to gap disturbance. We report a shift in species composition at the study site consisting of the replacement of seagrass by an extensive macroalgal cover. Succession patterns were tested in each zone by sampling macrophyte cover along transects running across gaps. Our results show that seagrass is always the first colonizer, independent of dominant cover in control plots. The reversal of competitive hierarchy described has important consequences for the understanding and management of seagrass ecosystems.

Introduction

For the past several decades, marine ecology has studied life history traits of various forms of seagrass attempts to explain the relative importance of these angiosperms in coastal ecosystems. Aside from being an important stabilizer of bottom sediments (Patriquin 1973, p. 111), seagrass provides the organic substrate needed for the establishment of epibionic fauna and a diverse assemblage of plants and animals (Aladro-Lubel & Martinez-Murillo 1999, p. 239). Since these communities develop rapidly, and are found in soft-bottomed coastal systems worldwide (Williams 1990, p. 450), it is important to understand the patterns of succession in seagrass beds as a way of explaining recovery processes after disturbances.

Ecological succession is defined as changes observed in an ecological community following a perturbation that opens up a relatively large space (Connell & Slatyer 1977, p. 1119). During successional sequences, the first species arriving in the disturbed area are called the primary colonizers. These species usually have poor competitive abilities, and rapid colonzation rates on bare sediments. These species are soon displaced from the system by the secondary colonizers. Secondary colonizers are strong competitors for resources with relatively slow colonization rates.

Disturbance, succession and recovery processes have been at mainstays in ecological theory since the early 1950s in terrestrial and marine systems. Their importance for understanding and managing natural ecosystems is well recognized. In a classic example, Mediterranean forest systems rely on frequent fire disturbances to maintain their structure and function through natural successional processes (Fernández-Abascal et al 2004, 147). In seagrass ecosystems, Den Hartog (1971) was the first to propose successional schemes based on competition-colonization hierarchies, with seagrass species as the climax of a sequence involving macroalgae and seagrasses.

This study examines succession dynamics in a wave-disturbed seagrass ecosystem located on the east coast of Barbados. The dominance of the seagrass Thalassia testudinum in this ecosystem was originally attributed by Patriquin (1975) to wave disturbances, which disrupt the seagrass matrix and create sharp topographic depressions known as gaps. These gaps are hypothesized to contribute to the maintenance of the subordinate seagrass species

Syringodium filiforme and of a subordinate algal species complex, Avrainvillea sp. in the seagrass bed. More recently, Tewfik et al. (in review) documented a historical shift in the species distribution within the ecosystem, showing that Avrainvillea has formed a dominant cover in a region (40m wide and 45m offshore) previously occupied by seagrass. This species shift could potentially contradict the established model for the competitive hierarchy in seagrass communities.

The general goal of our study is to present a model for the species shift and the maintenance of extensive cover of Avrainvillea by examining the complex successional patterns within a wave-disturbed seagrass community. Assuming that gaps migrate and that patterns of species composition in their trail can inform us about spatial and temporal successional sequences, the following hypotheses were tested: (1) Avrainvillea is a dominant species and its cover varies in relation to physical gradients and (2) recovery and disturbance intensities are explained by offshore and alongshore physical gradients (hydrodynamics and biomass loss).

Materials and Methods

The experimental part of this study was carried out at Bath, Barbados during May and June of 2004 (Fig. 2B). The seagrass site under investigation is 100m wide and 120m long (Fig. 2A). Gaps were defined as sharp topographic depressions created by wave disturbance, over 0.2m deep and not less than 3m wide. All gaps fitting these criteria found between 10-30m and 60-80m alongshore and offshore were mapped and measured. These gaps were also pegged at four different points (scarp, beginning of leeward slope, and left and right edges) in order to measure their migration rate over 30 days. Succession sequences were characterized by measuring the percentage surface cover for each species using 1m2 quadrants at every meter along a 17m transect running offshore from 4m before to 12m after the scarp of each gap. Control transects were sampled at 2m from the right and left edges of each gap (Fig. 2C).

Results and Discussion

Our study reveals three distinct zones. Zone I is composed of seagrass Thalassia testudinum and Syringodium filiforme, Zone II is mainly occupied by the macroalgae Avrainvillea, and offshore Zone III is a mixed assemblage of seagrasses and macroalgae. The macroalgal zone documented here results from a historical (<30 years) shift from the original mixed assemblage documented by Patriquin (1975). The data was filtered for the interactions between seagrass species and Avrainvillea, present exclusively in Zones II and III.

At the scale of individual gaps, we were able to analyze a temporal successional sequence from spatial transects sampled across migrating gaps (Fig. 3). In contrast with previous studies, we showed that seagrass species are the first colonizers after disturbance, irrespective of the surrounding dominant cover. Avrainvillea progressively replaces the strong competitor seagrass species. Furthermore, Avrainvillea recovery is slower in the mixed zone compared to the macroalgal zone. These results suggest that disturbance dynamics, rather than an equilibrium succession endpoint, prevent the full recovery of Avrainvillea, and maintain the mixed assemblage observed in the offshore zone.

Conclusion

Our results failed to support den Hartog's (1971) successional sequence, which established macroalgae as the first subordinate colonizers and seagrasses as the climax species (Fig. 1A). The reversal of competitive hierarchy shown here (Fig. 1B) will have important consequences for the understanding and management of seagrass ecosystems. Future research should examine the underlying processes explaining the large-scale historical shifts from seagrass to macroalgal assemblages, in light of our results establishing Avrainvillea as the potential endpoint of succession.

Acknowledgements

We would like to thank the Bellairs Research Institute of McGill University at Barbados for the provision of the laboratory and field equipment used during our data collection. We would also like to thank Diorys Pérez for her valuable assistance during fieldwork at Bath, Barbados. Finally we want to thank Alexander Tewfik for his comments during our discussions of the project.

References

1. Aladro-Lubel, M. A., and Martinez-Murillo, M. E. 1999. Epibiotic Protozoa (Ciliophora) on a community of Thalassia testudinum Banks ex Konig in a coral reef in Veracruz, Mexico. Aquatic Botany 65 (1-4):**239-254**.

2. Connell, J. H., and Slatyer, R. O. 1977. Mechanisms of Succession in Natural Communities and Their Role in Community Stability and Organization. The American Naturalist 111 (982):**1119-1144**.

3. Fernandez-Abascal, I., Reyes T., and Luis-Calabuig, E. 2004. Ten years of recovery after experimental fire in a heathland: effects of sowing native species. Forest Ecology and Management 203 (1-3):**147-156**.

4. Patriquin, D. G. 1973. Estimation of growth rate, production and age of the marine angiosperm Thalassia testudinum Konig. Caribbean Journal of Science 13 (1-2):**111-123**.

5. ———. 1975. "Migration" of blowouts in seagrass beds at Barbados and Carriacou, West Indies, and its ecological and geological implications. Aquatic Botany 1:**163-189**.

6. Tewfik, A., Guichard, F., and McCann, K. S. in review. Acute and chronic physical disturbance facilitates landscape zonation and species composition within a tropical macrophyte bed.

7. Williams, S. L. 1990. Experimental Studies of Caribbean Seagrass Bed Development. Ecological Monographs 60 (4):**449-469**.

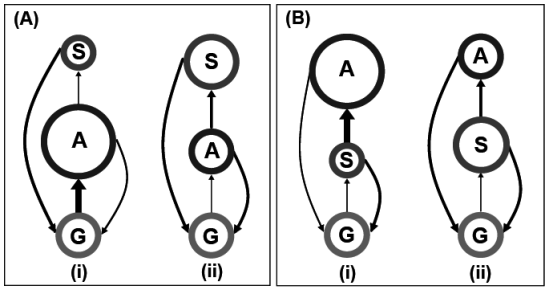

Figure 1. Schematic representation of the two conflicting hypotheses, where G: gap, A: Avrainvillea and S: seagrass. The size of the circle symbolizes the abundance of each species during succession and the size of the arrows the strength of the transition from one state to the other.

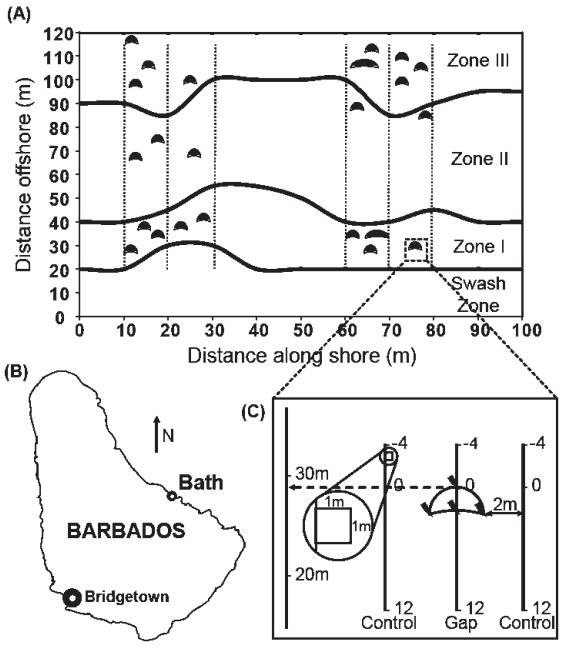

Figure 2. Sampling design. (A) Study site map with all the gaps and transects, (B) Map of Barbados, (C) Close up of a pegged gap describing the vegetation sampling design: 2 control, 1 gap transect and a 1m^2 quadrant are depicted. Extreme left line depicts the transect used to map the gap on the site.

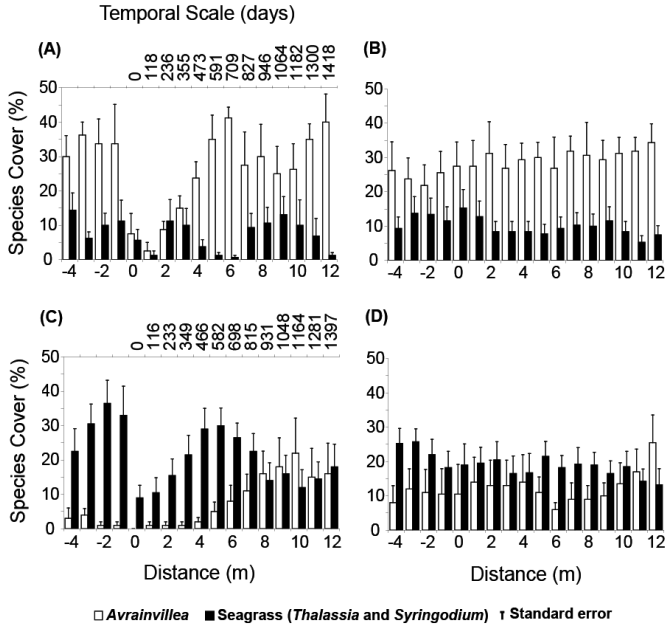

Figure 3. Gap (A & C) and control (B & D) profiles for Zone II (Macroalgae) and Zone III (Mixed) respectively. The gap profile depicts both the spatial and temporal successional sequences and shows how the species abundance changes over time after gap creation (distance = 0m). Comparisons of species abundance can be made with the control profiles that are devoid of disturbances.

Special Thanks

The McGill Science Undergraduate Research Journal would not have been possible if not for the tireless dedication, sacrifice, hard work and vision of our staff throughout the process. These people have shown tremendous leadership and are an inspiration for research excellence.

Editorial Board Members:

Aaron Besterman
Adam Parent
Sarah Barama
Victor Tremblay
Sapna Mahajan
Katie Young
James Curtis
Daniel Spitzberg
Christine Matte
Ariella Zbar
Naila Karim

Dr. David Harpp

A special thanks also goes to someone, without whom our vision would only be a thought. Alyson Lockwood is responsible for the amazing layout and design of the Journal. The MSURJ team thanks you for all of your hard work.

Claudio Calligaris for McGill Faculty of Science

ISSN 1718-0775

MSURJ
McGill Science Undergraduate Research Journal
Burnside Hall, Rm. 1B21
805 Sherbrooke St. W.
Montreal, Quebec H3A 2K6
Canada
p. (514) 398 6979 : f. (514) 398 6766
mcgillsruj@gmail.com : www.msurj.mcgill.ca